

## Supporting Information

### Orientation of $\alpha$ -CD component of [2]rotaxanes affects their specific molecular recognition behaviour

Takuya Iwamoto, Shinobu Miyagawa, Masaya Naito and Yuji Tokunaga

#### Table of contents

<b>Experimental</b>	1
<b>Figure S1.</b> $^1\text{H}$ NMR spectral titration of compound <b>5b</b> with $\alpha$ -CD.	3
<b>Figure S2.</b> $^1\text{H}$ NMR spectra of the [2]rotaxanes <b>1</b> and <b>2</b> and the dumbbell-shaped molecule <b>6</b> .	4
<b>Figure S3.</b> HPLC analysis of a mixture of the [2]rotaxanes <b>1</b> and <b>2</b> .	5
<b>Figure S4.</b> 2D NMR spectra of the [2]rotaxane <b>1</b> .	6
<b>Figure S5.</b> 2D NMR spectra of the [2]rotaxane <b>2</b> .	10
<b>Figure S6.</b> $^1\text{H}$ NMR spectra of the [2]rotaxane <b>1</b> in the presence of $\text{Bu}_4\text{NOAc}$ ; determination of the association constant for <b>1</b> and the $\text{AcO}^-$ anion using BindFit.	14
<b>Figure S7.</b> $^1\text{H}$ NMR spectra of the [2]rotaxane <b>2</b> in the presence of $\text{Bu}_4\text{NOAc}$ .	16
<b>Figure S8.</b> $^1\text{H}$ NMR spectra of the dumbbell-shaped molecule <b>6</b> in the presence of $\text{Bu}_4\text{NOAc}$ ; determination of the association constant of <b>6</b> and the $\text{AcO}^-$ anion by BindFit.	17
<b>Figure S9.</b> UV–Vis absorption spectra of the dumbbell-shaped molecule <b>6</b> in the presence of $\text{Bu}_4\text{NOAc}$ in $\text{CH}_3\text{CN}/\text{DMSO}$ (9:1).	19
<b>Figure S10.</b> UV–Vis absorption spectra of the [2]rotaxanes <b>1</b> and <b>2</b> and the dumbbell-shaped molecule <b>6</b> in the presence of $\text{Bu}_4\text{NOH}$ in $\text{CH}_3\text{CN}/\text{DMSO}$ (9:1).	20
<b>Figure S11.</b> UV–Vis absorption spectra of the [2]rotaxanes <b>1</b> and <b>2</b> and the dumbbell-shaped molecule <b>6</b> in the presence of $\text{Bu}_4\text{NOMs}$ in $\text{CH}_3\text{CN}/\text{DMSO}$ (9:1).	21
<b>Figure S12.</b> $^1\text{H}$ NMR spectra of the [2]rotaxane <b>1</b> in the presence of $\text{Bu}_4\text{NOMs}$ ; determination of the association constant for <b>1</b> and the $\text{MsO}^-$ anion using BindFit.	22
<b>Figure S13.</b> $^1\text{H}$ NMR spectra of the [2]rotaxane <b>2</b> in the presence of $\text{Bu}_4\text{NOMs}$ ;	

determination of the association constant for **2** and the  $\text{MsO}^-$  anion using BindFit.

23

**Figure S14.**  $^1\text{H}$  NMR spectra of the dumbbell-shaped molecule **6** in the presence of  $\text{Bu}_4\text{NOMs}$ ; determination of the association constant for **6** and the  $\text{MsO}^-$  anion using BindFit.

24

**Figure S15.** UV–Vis absorption spectra of the [2]rotaxanes **1** and **2** and the dumbbell-shaped molecule **6** in  $\text{CH}_3\text{CN/DMSO}$  (9:1) and  $\text{H}_2\text{O/DMSO}$  (9:1).

25

**Figure S16.** UV–Vis absorption spectra of the [2]rotaxanes **1** and **2** and the dumbbell-shaped molecule **6** in the presence of  $\text{Bu}_4\text{NOAc}$  in  $\text{H}_2\text{O/DMSO}$  (9:1).

26

**Figure S17.**  $^1\text{H}$  and  $^{13}\text{C}$  NMR spectra of compound **3**.

27

**Figure S18.**  $^1\text{H}$  and  $^{13}\text{C}$  NMR spectra of compound **4**.

28

**Figure S19.**  $^1\text{H}$  and  $^{13}\text{C}$  NMR spectra of compound **5a**.

29

**Figure S20.**  $^1\text{H}$  and  $^{13}\text{C}$  NMR spectra of compound **5b**.

30

**Figure S21.**  $^1\text{H}$  and  $^{13}\text{C}$  NMR spectra of the [2]rotaxane **1**.

31

**Figure S22.**  $^1\text{H}$  and  $^{13}\text{C}$  NMR spectra of the [2]rotaxane **2**.

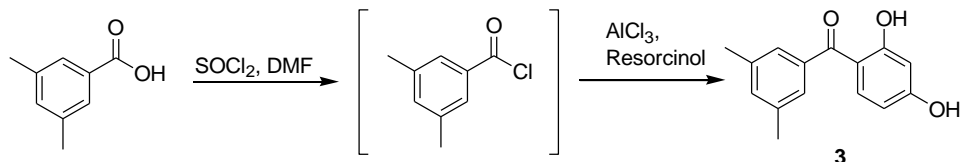
32

**Figure S23.**  $^1\text{H}$  and  $^{13}\text{C}$  NMR spectra of the dumbbell-shaped molecule **6**.

33

## Experimental

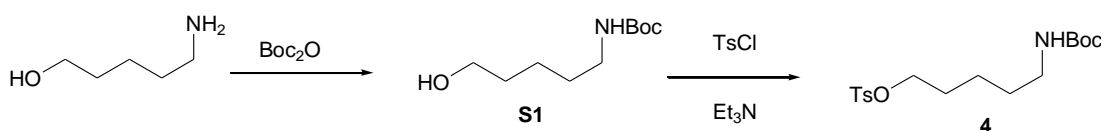
### 2,4-Dihydroxy-3',5'-dimethylbenzophenone (**3**)



$\text{SOCl}_2$  (12.0 mL) and DMF (1 drop) were added to 3,5-dimethylbenzoic acid (3.00 g, 20.0 mmol) and then the mixture was heated under reflux overnight. Evaporation of the excess  $\text{SOCl}_2$  and DMF gave the crude acid chloride, which was dissolved in nitrobenzene (70 mL) and added to a suspension of resorcinol (2.97 g, 27 mmol) and  $\text{AlCl}_3$  (10.7 g, 80 mmol) in nitrobenzene (40 mL) at 0 °C. The mixture was heated at 65 °C overnight. After cooling, the mixture was treated with 10% HCl (aq) (80 mL) and filtered through Celite. The organic phase of the filtrate was separated, washed with water and sat. NaCl (aq), dried ( $\text{Na}_2\text{SO}_4$ ), and concentrated (nitrobenzene was evaporated through distillation). The solid residue was washed with hexane to afford a pale-yellow solid (2.95 g, 54%).  $^1\text{H}$  NMR (600 MHz, acetone- $d_6$ )  $\delta$ : 2.35 (s, 6H), 6.38–6.41 (m, 2H), 7.21 (br s, 2H), 7.23 (br s, 1H), 7.49 (d,  $J = 8.0$  Hz, 1H), 9.70 (br s, 1H), 12.67 (s, 1H).  $^{13}\text{C}$  NMR (125 MHz, acetone- $d_6$ )  $\delta$ : 21.2, 103.7, 108.6, 113.3, 127.1, 133.6, 136.8, 138.7, 139.3, 165.8, 167.1, 201.0.

The  $^1\text{H}$  and  $^{13}\text{C}$  NMR spectra of **3** were identical to those reported previously.<sup>1</sup>

### 5-(*N*-*tert*-Butoxycarbonylamino)-1-pentyl *p*-Toluenesulfonylate (**4**)



A solution of 5-amino-1-pentanol (3.10 g, 30.0 mmol) and di-*tert*-butyl dicarbonate (7.20 g, 33.0 mmol) in tetrahydrofuran (THF; 20 mL) was stirred overnight at room temperature. After evaporation of the solvent, the residue was dissolved in EtOAc. The solution was washed with water and sat. NaCl (aq), dried ( $\text{Na}_2\text{SO}_4$ ), and concentrated to afford the crude carbamate **S1**. Tosyl chloride (6.86 g, 36 mmol) was added portionwise to a solution of crude **S1**,  $\text{Et}_3\text{N}$  (4.55 g, 45.0 mmol), and *N,N*-dimethylaminopyridine (DMAP; 367 mg, 3.00 mmol) in  $\text{CH}_2\text{Cl}_2$  (40 mL) at 0 °C. After stirring for 4 h at room temperature, the mixture was treated with water and the aqueous phase extracted with  $\text{CH}_2\text{Cl}_2$ . The combined extracts were washed with water and sat. NaCl (aq), dried ( $\text{Na}_2\text{SO}_4$ ), and concentrated. The residue was chromatographed ( $\text{SiO}_2$ ; hexane/EtOAc,

2:1) to give a white solid (8.96 g, 84%).  $^1\text{H}$  NMR (500 MHz,  $\text{CDCl}_3$ )  $\delta$ : 1.30–1.37 (m, 2H), 1.39–1.48 (m, 11H), 1.62–1.70 (m, 2H), 2.46 (s, 3H), 3.01–3.11 (m, 2H), 4.02 (t,  $J = 6.3$  Hz, 2H), 4.48 (br s, 1H), 7.35 (d,  $J = 8.3$  Hz, 2H), 7.79 (d,  $J = 8.3$  Hz, 2H).  $^{13}\text{C}$  NMR (125 MHz,  $\text{CDCl}_3$ )  $\delta$ : 21.6, 22.6, 28.3, 28.4, 29.3, 40.1, 70.3, 79.0, 127.8, 129.8, 133.0, 144.7, 155.9.

The  $^1\text{H}$  and  $^{13}\text{C}$  NMR spectra of **4** were identical to those reported previously.<sup>2</sup>

#### References

1. N. A. Serratore, C. B. Anderson, G. B. Frost, T.-G. Hoang, S. J. Underwood, P. M. Gemmel, M. A. Hardy, C. J. Douglas, *J. Am. Chem. Soc.*, 2018, **140**, 10025–10033.
2. L. A. Webster, M. Thomas, M. Urbaniak, S. Wyllie, H. Ong, M. Tinti, A. H. Fairlamb, M. Boesche, S. Ghidelli-Disse, G. Drewes, I. H. Gilbert, *ACS Infect. Dis.*, 2018, **4**, 1475–1486.

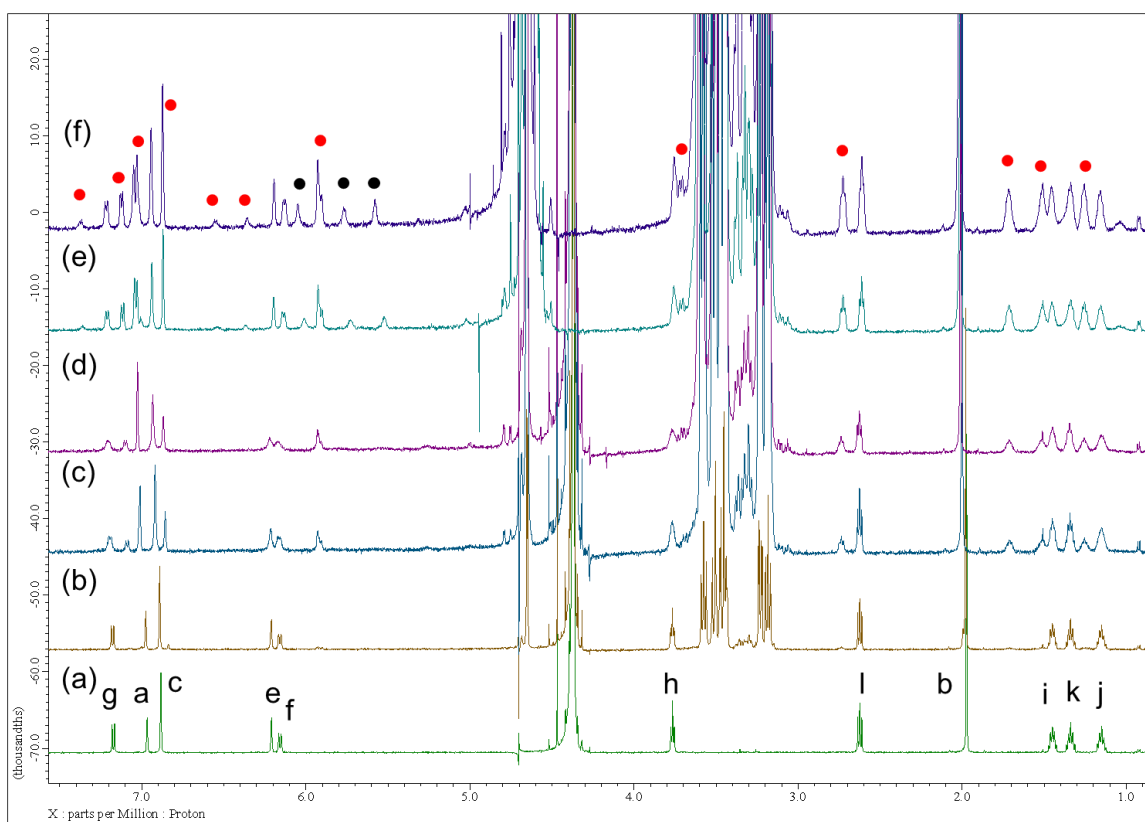


**Figure S1.**  $^1\text{H}$  NMR spectra (600 MHz,  $\text{D}_2\text{O}$ ) of mixtures of **5b** (1 mM) and  $\alpha\text{-CD}$  (0–10 eq). (a) **5b** at 25 °C, (b) mixture of **5b** and  $\alpha\text{-CD}$  (1 eq) at 25 °C, (c) mixture of **5b** and  $\alpha\text{-CD}$  (6 eq) at 25 °C, (d) mixture of **5b** and  $\alpha\text{-CD}$  (10 eq) at 25 °C, (e) sample (d) at 5 °C, (f) sample (d) at 1 °C. Red circle: pseudorotaxanes; ●:  $\alpha\text{-CD}$ . Partial spectra of Figure S1 are shown in Figure 2.

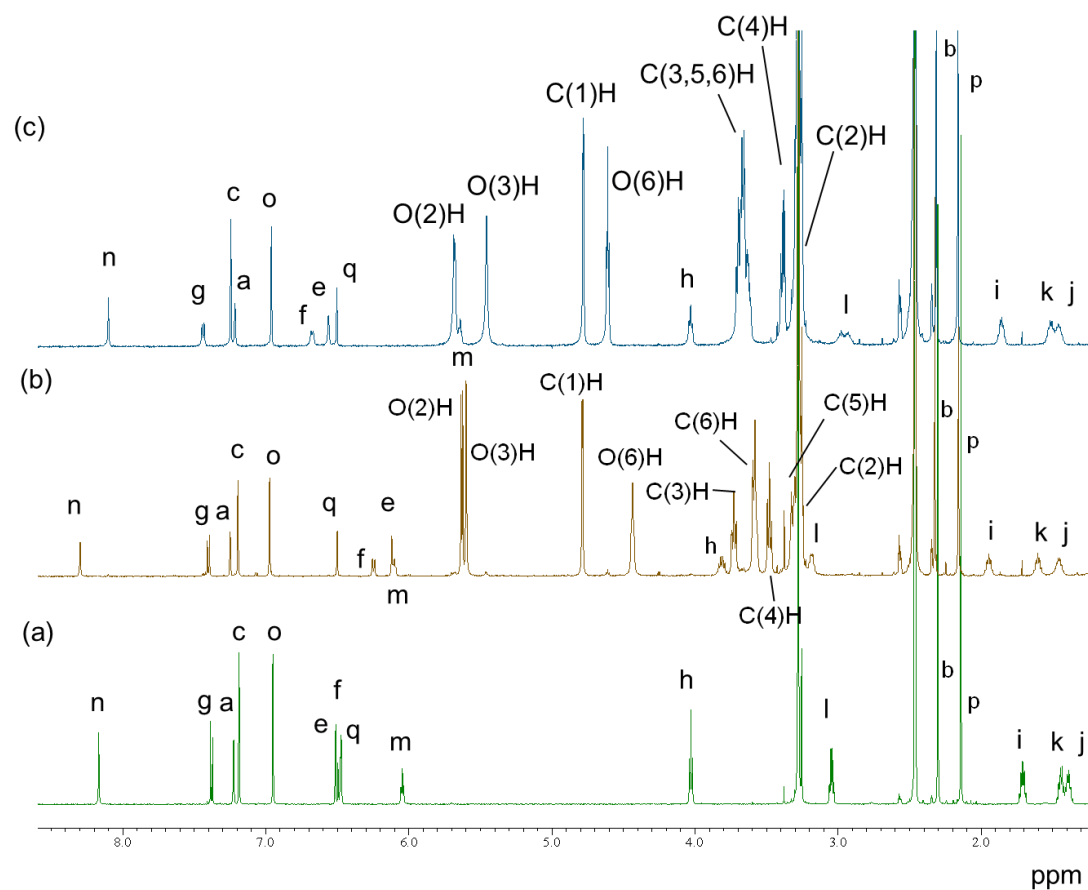
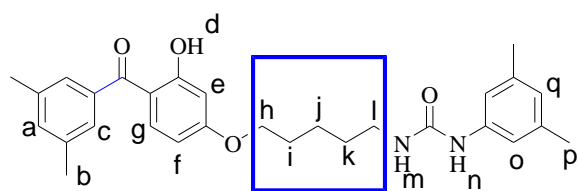


**Figure S2.**  $^1\text{H}$  NMR spectra (600 MHz,  $\text{DMSO-}d_6$ , 25  $^\circ\text{C}$ ) of (a) the dumbbell-shaped molecule **6**, (b) the [2]rotaxane **1**, and (c) the [2]rotaxane **2**.

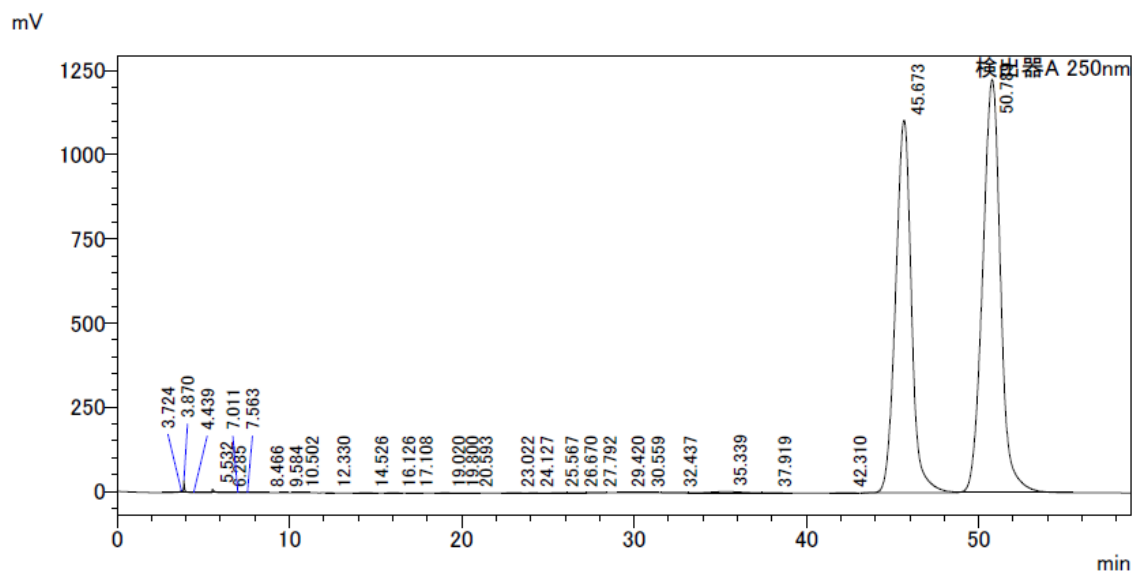


**Figure S3.** HPLC analysis of the [2]rotaxanes **1** and **2**. Peaks at 45 and 50 min are assigned to the [2]rotaxanes **1** and **2**, respectively.

#### HPLC conditions

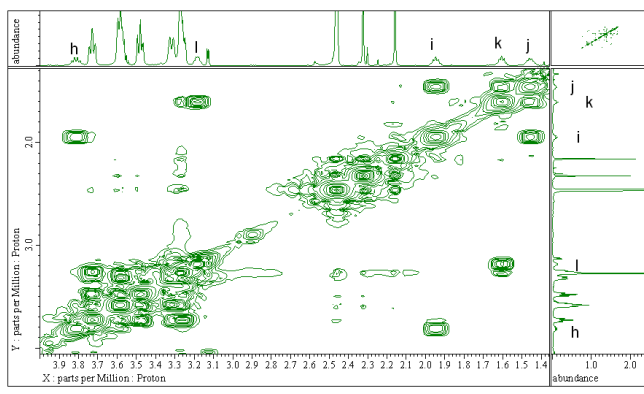
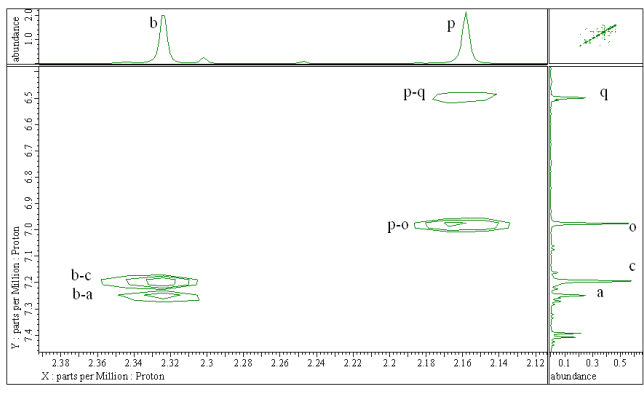
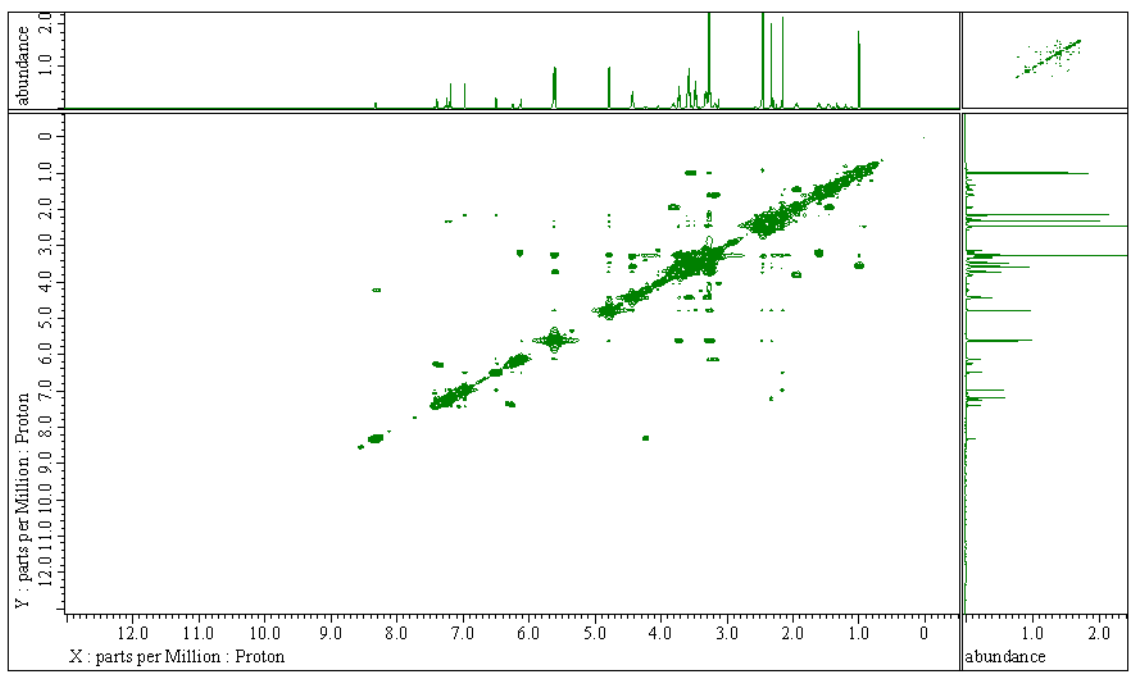
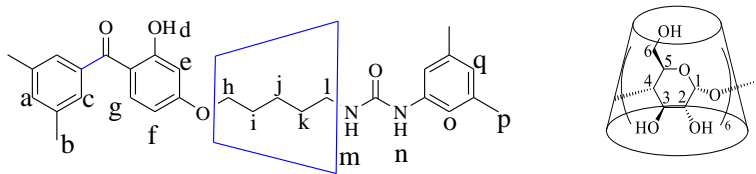
Column: Wako Wakosil-II 5C18 HG Prep (20 mm × 250 mm)

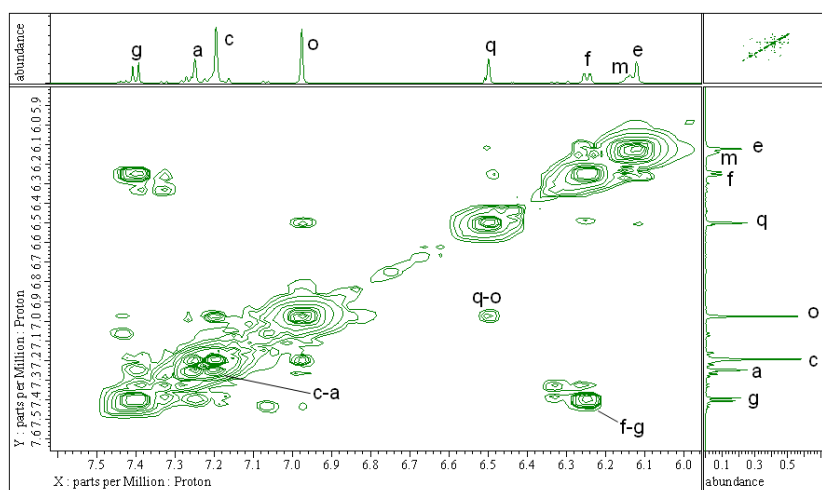
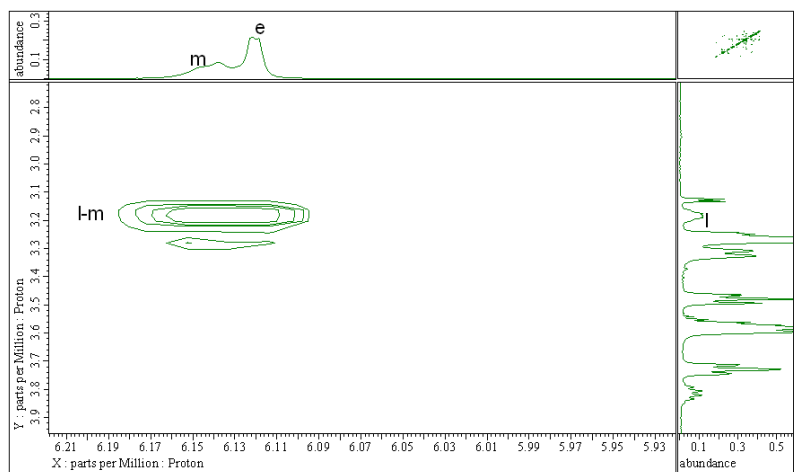
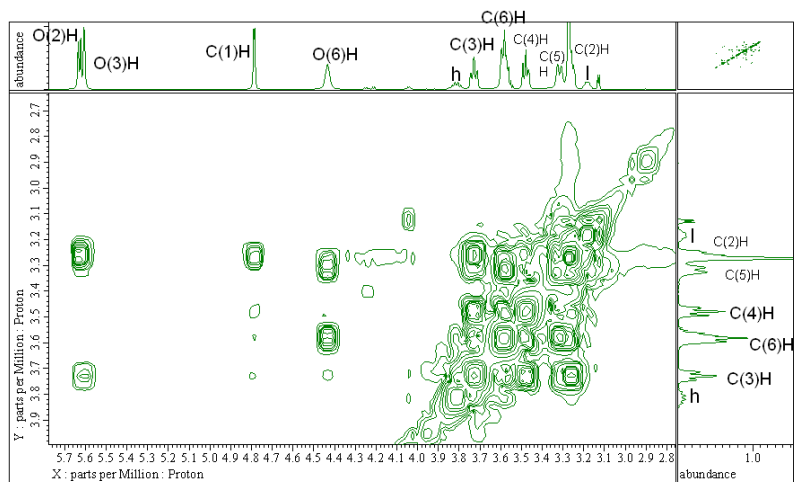
Eluent: Water/MeCN (4:1)

Flow rate: 12 mL/min

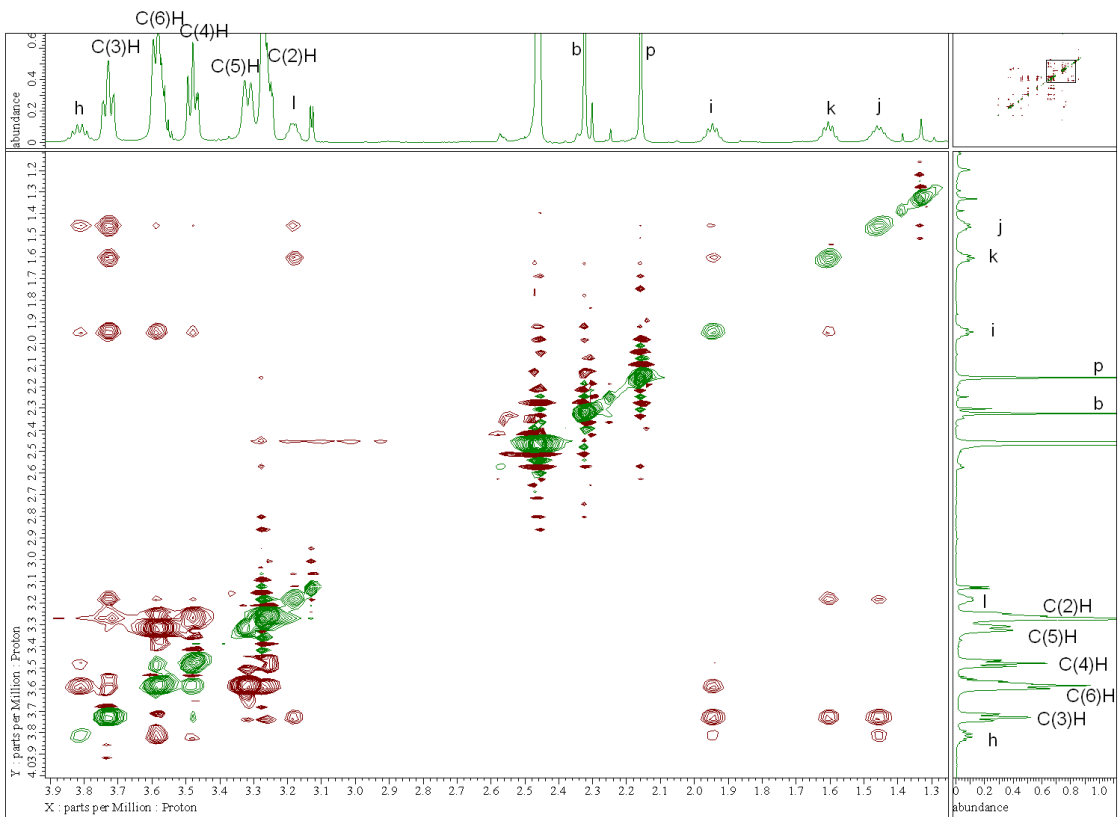
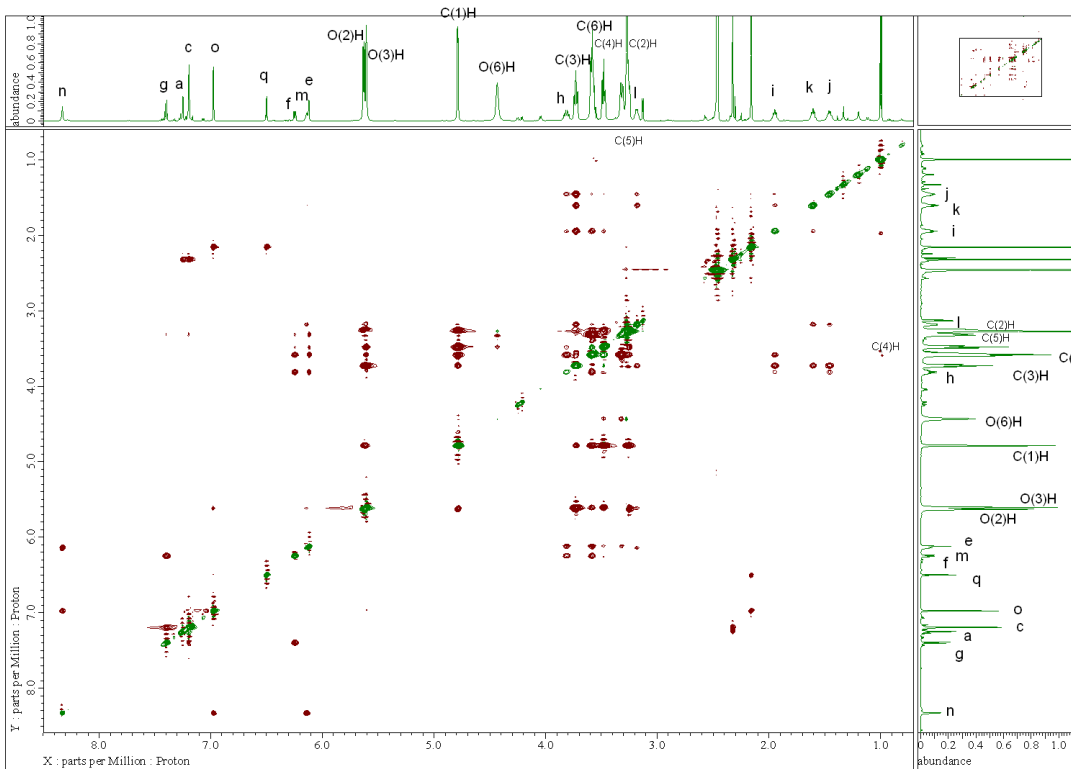
Temperature: ambient temp.

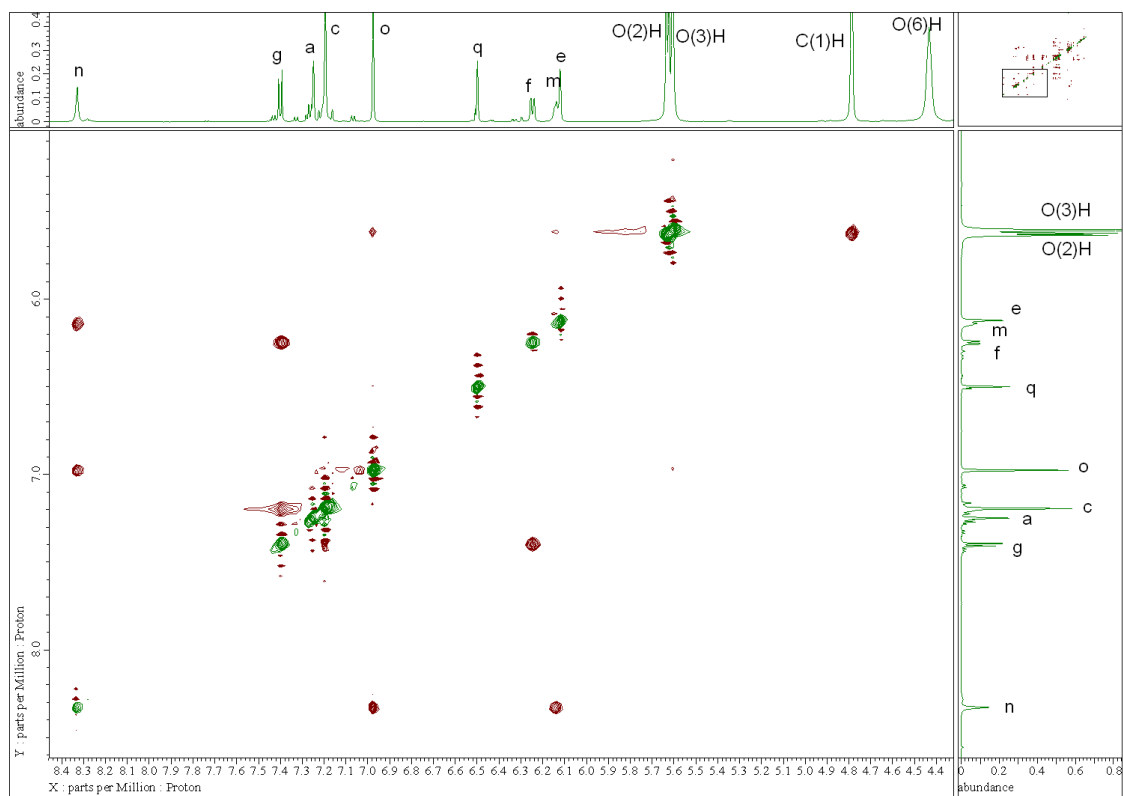
Detection: 250 nm (UV)



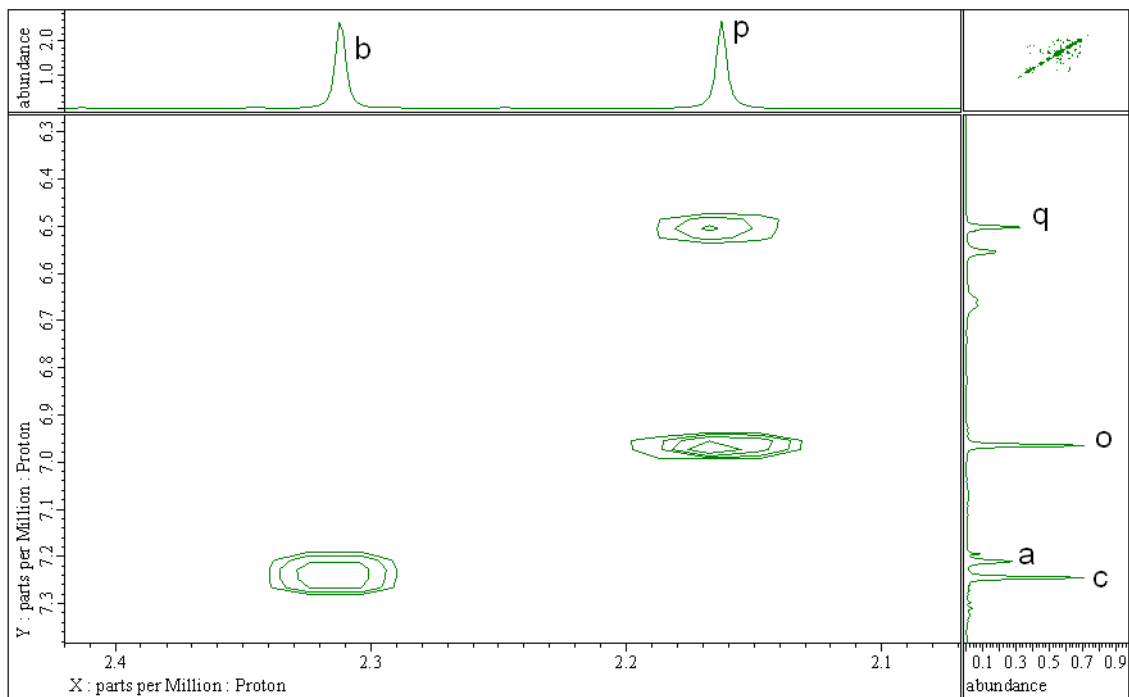
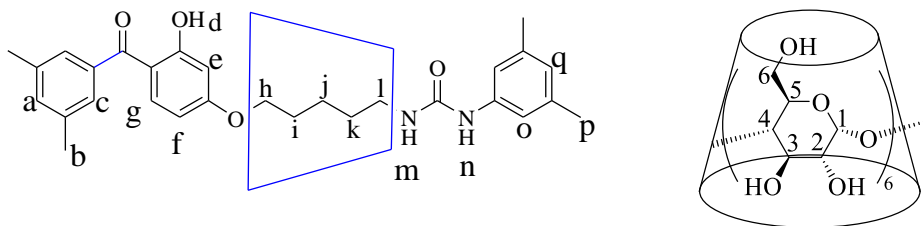


**Figure S4a.** COSY spectrum (600 MHz, DMSO-*d*<sub>6</sub>, 25 °C) of the [2]rotaxane **1**.





**Figure S4b.** ROESY spectrum (600 MHz, DMSO-*d*<sub>6</sub>, 25 °C) of the [2]rotaxane **1**.



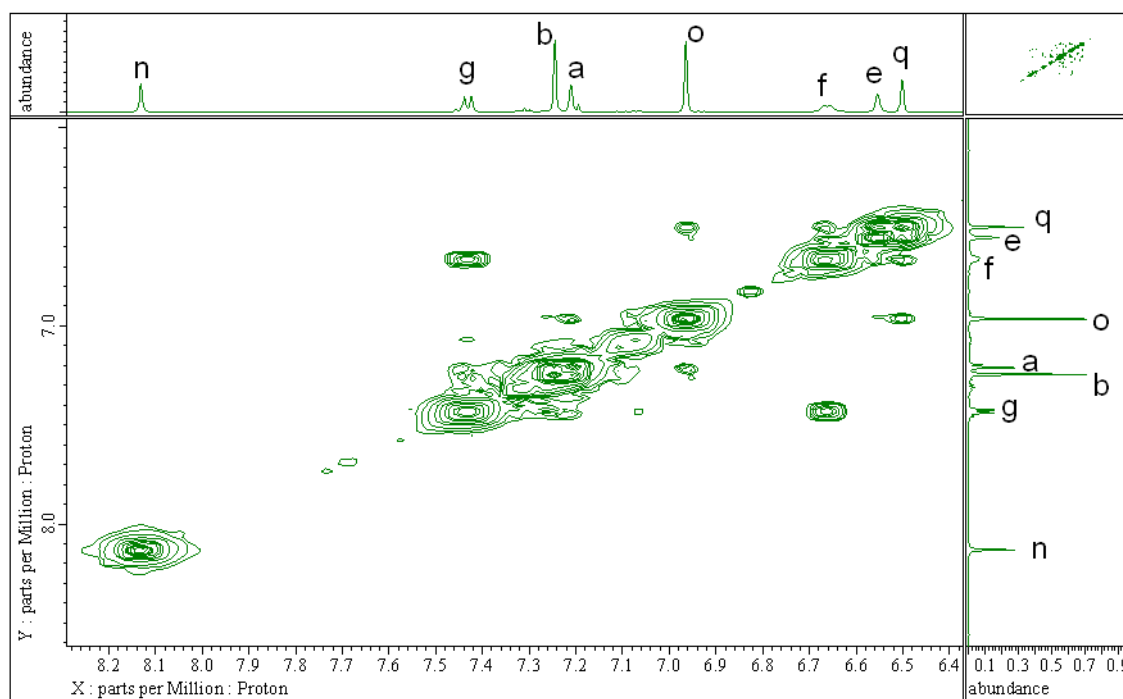
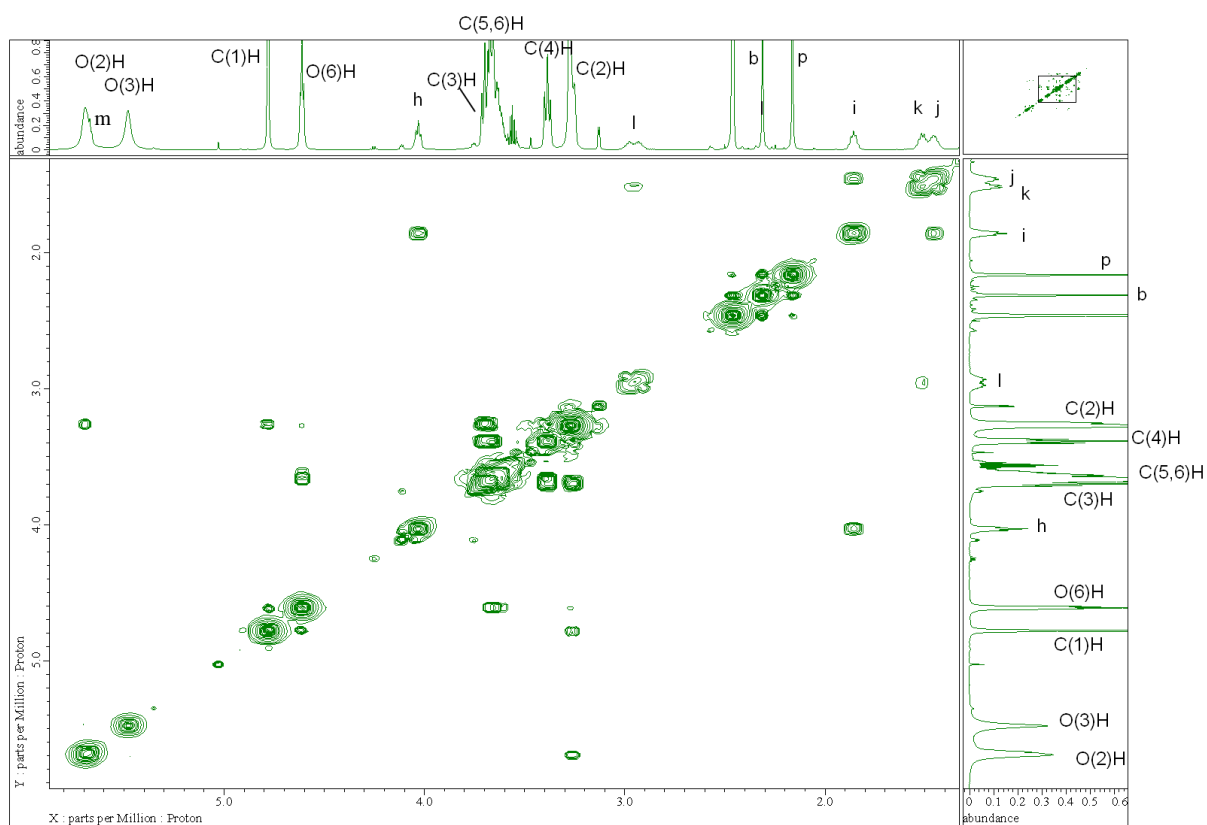


**Figure S5a.** COSY spectrum (600 MHz, DMSO-*d*<sub>6</sub>, 25 °C) of the [2]rotaxane **2**.



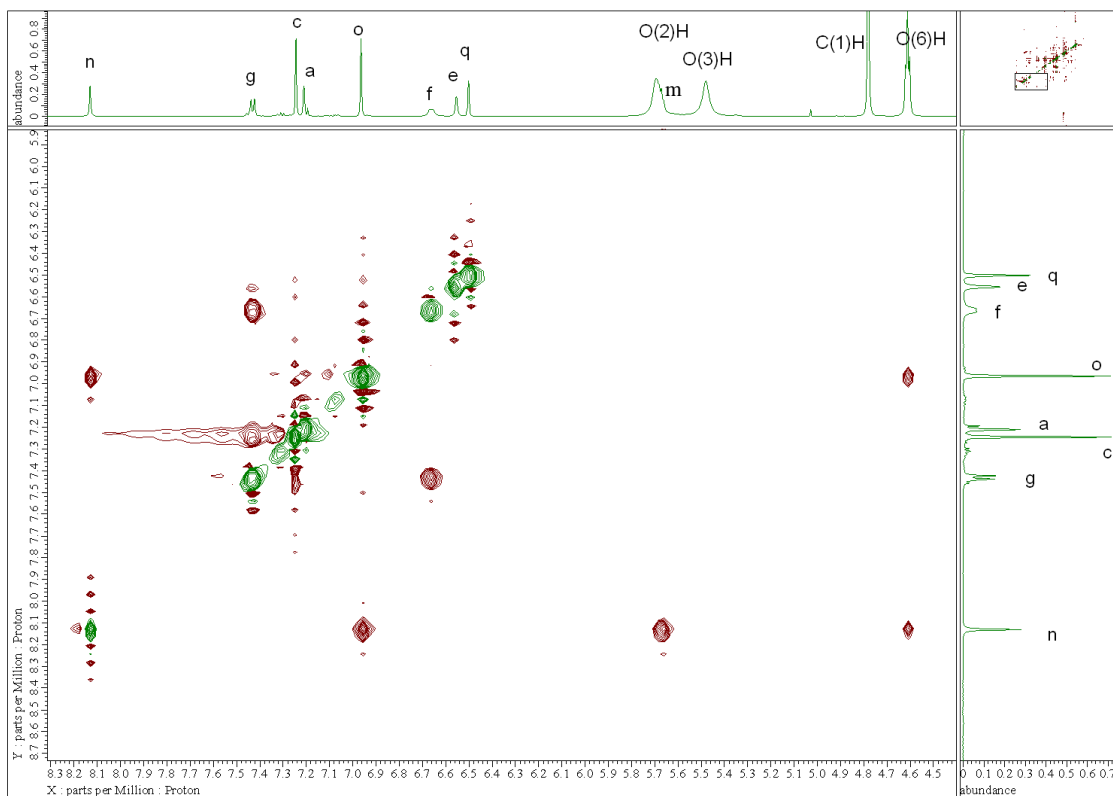


**Figure S5b.** ROESY spectrum (600 MHz, DMSO- $d_6$ , 25 °C) of the [2]rotaxane **2**.

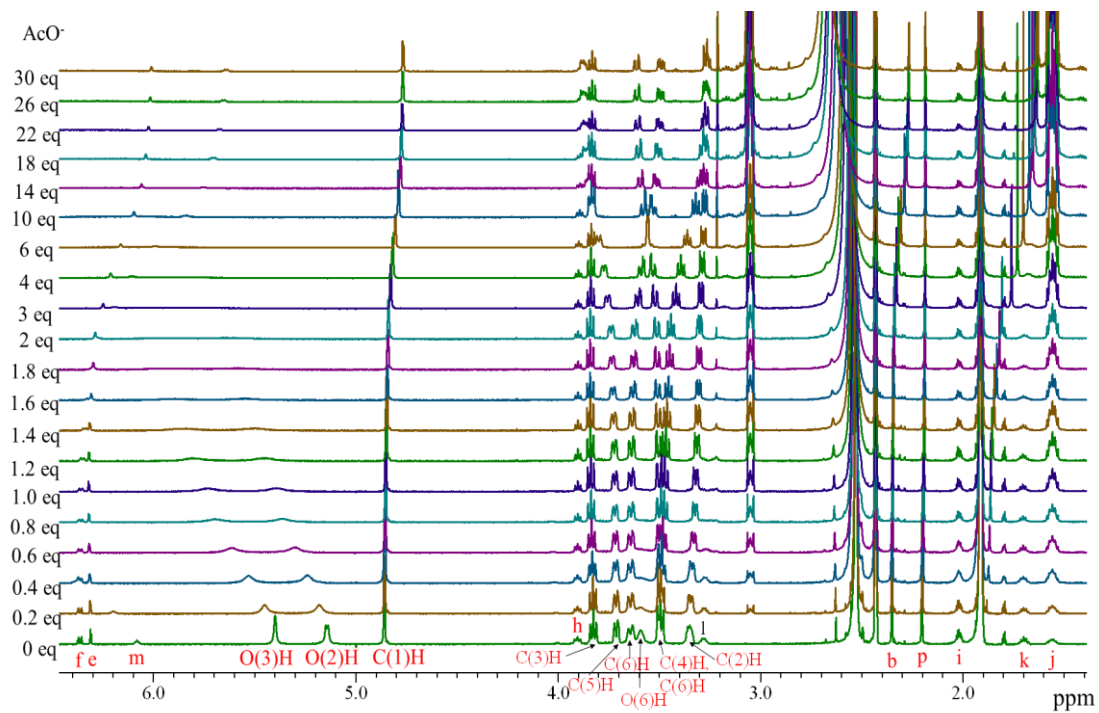
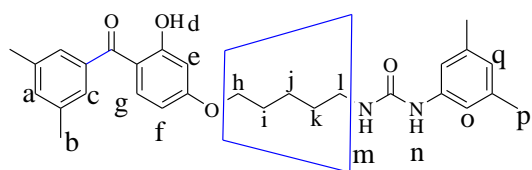


**Figure S6a.** Partial  $^1\text{H}$  NMR spectra [600 MHz,  $\text{CD}_3\text{CN}/\text{DMSO}-d_6$  (9:1), 25  $^\circ\text{C}$ ] of mixtures of the [2]rotaxane **1** (0.5 mM) and  $\text{Bu}_4\text{NOAc}$  (0–30 eq).

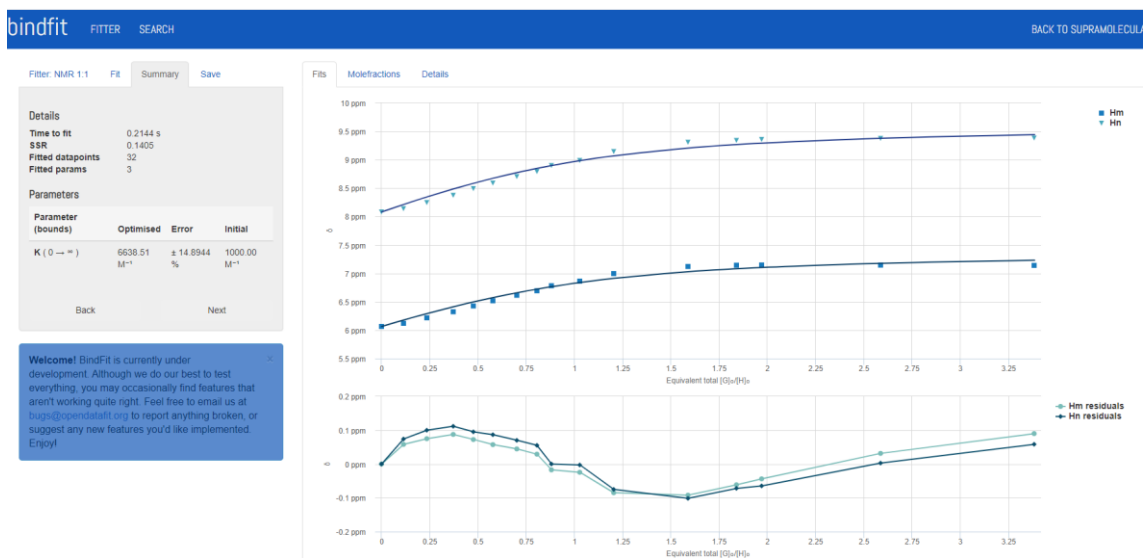
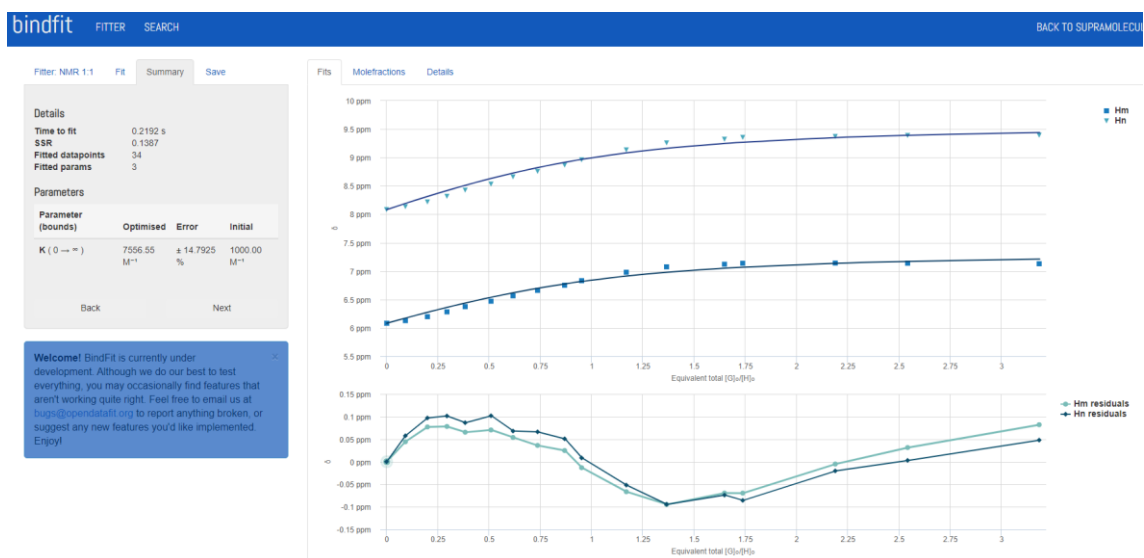


**Figure S6b.** Simulation of titrations of the [2]rotaxane **1** and Bu<sub>4</sub>NOAc using BindFit. The NMR titration experiments were performed twice.

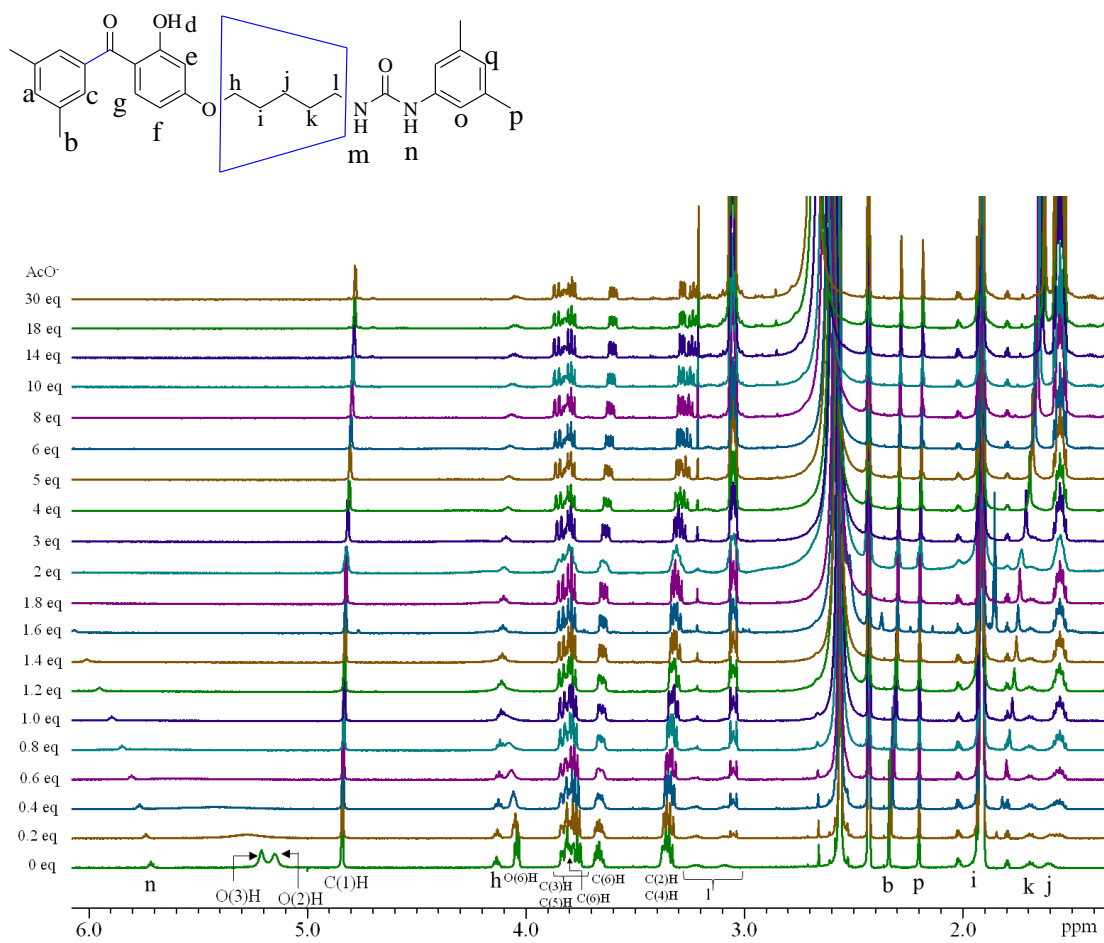


**Figure S7.** Partial <sup>1</sup>H NMR spectra [600 MHz, CD<sub>3</sub>CN/DMSO-*d*<sub>6</sub> (9:1), 25 °C] of mixtures of the [2]rotaxane **2** (0.5 mM) and Bu<sub>4</sub>NOAc (0–30 eq).

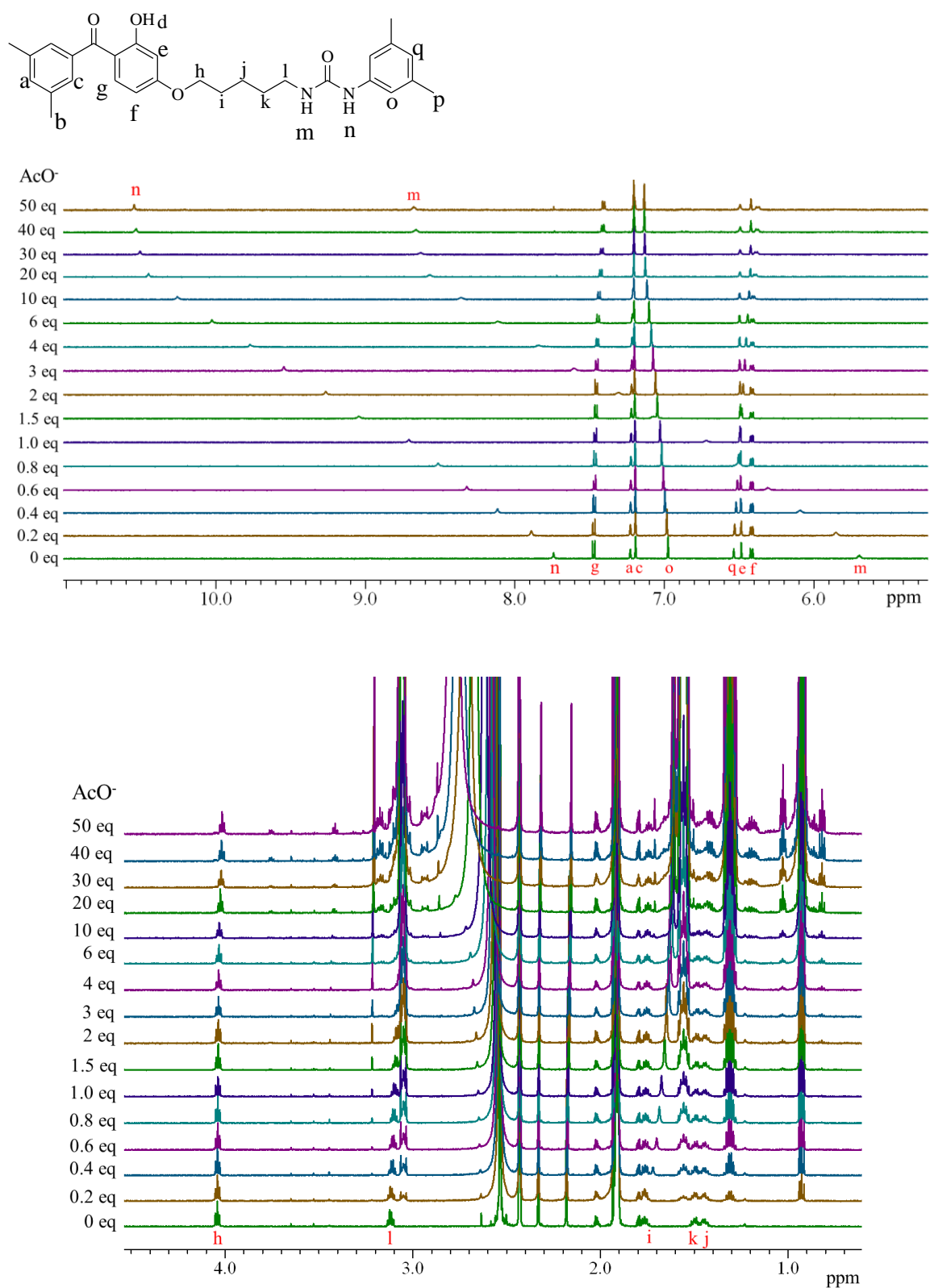


**Figure S8a.** Partial <sup>1</sup>H NMR spectra [600 MHz, CD<sub>3</sub>CN/DMSO-*d*<sub>6</sub> (9:1), 25 °C] of the dumbbell-shaped molecule **6** (0.5 mM) in the presence of Bu<sub>4</sub>NOAc (0–50 eq).

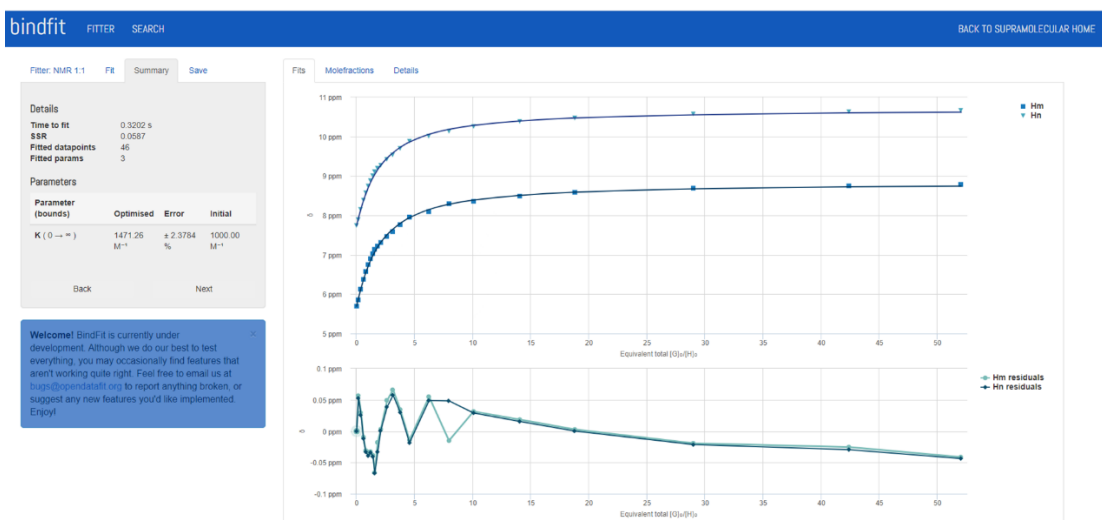
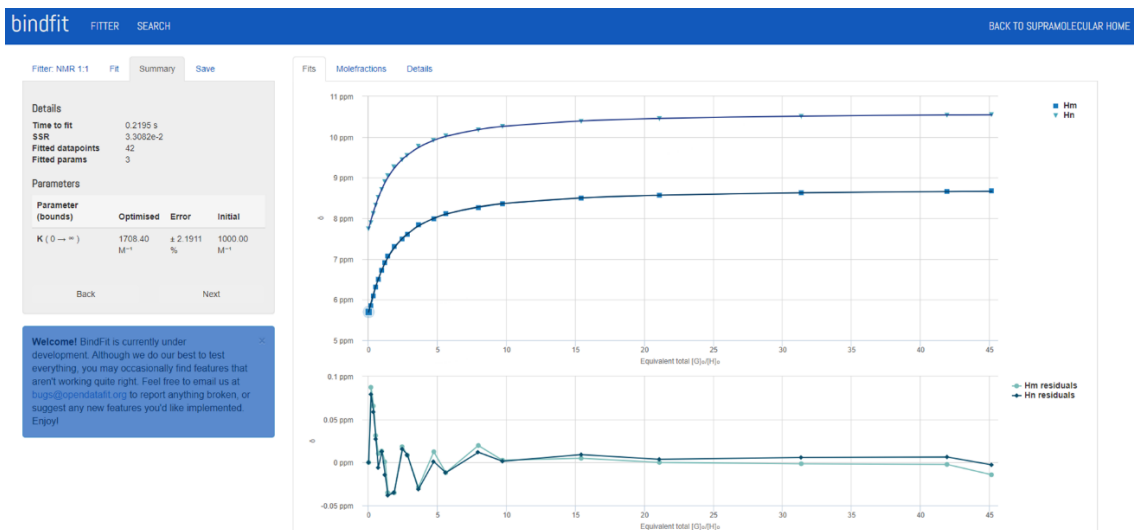


**Figure S8b.** Simulation of titrations of the dumbbell-shaped molecule **6** and Bu<sub>4</sub>NOAc using BindFit. The NMR titration experiments were performed twice.

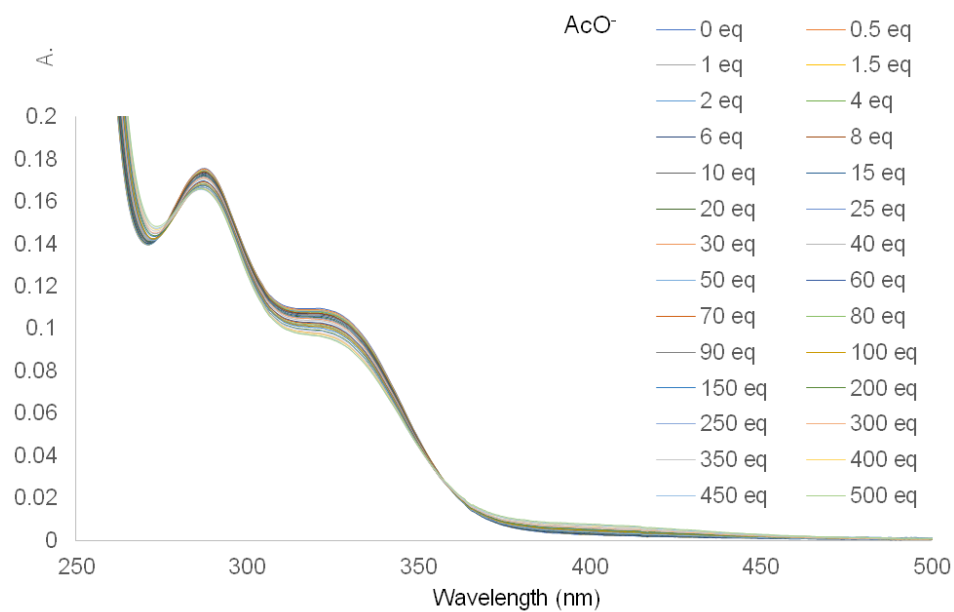


**Figure S9.** UV/Vis absorption spectra of the dumbbell-shaped molecule **6** [10 μM in CH<sub>3</sub>CN/DMSO (9:1), room temperature] in the presence of Bu<sub>4</sub>NOAc (0–500 eq).

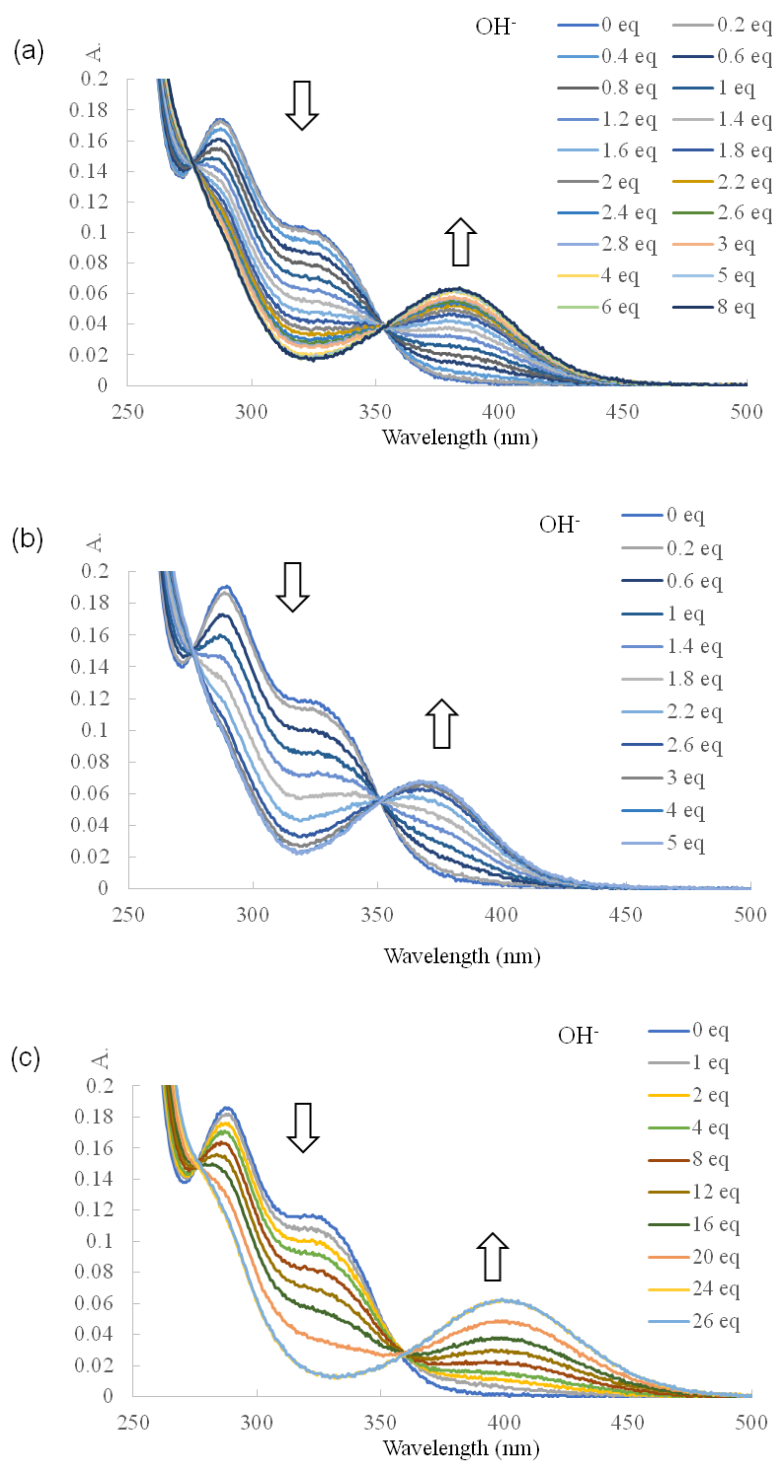


**Figure S10.** UV/Vis absorption spectra [10  $\mu$ M, CH<sub>3</sub>CN/DMSO (9:1), room temperature] of (a) the [2]rotaxane **1** in the presence of Bu<sub>4</sub>NOH (0–8 eq), (b) the [2]rotaxane **2** in the presence of Bu<sub>4</sub>NOH (0–5 eq), and (c) the dumbbell-shaped molecule **6** in the presence of Bu<sub>4</sub>NOH (0–26 eq).

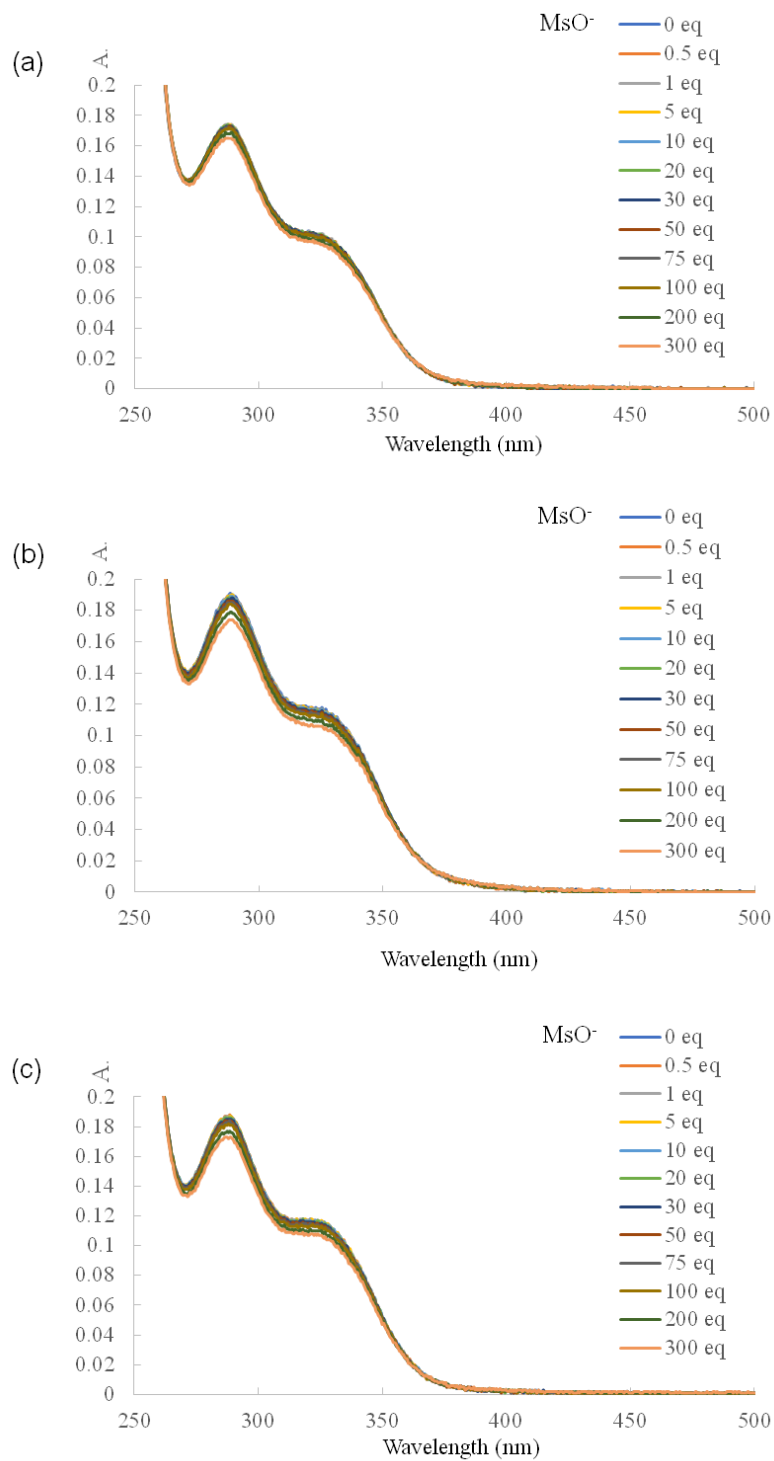


**Figure S11.** UV/Vis absorption spectra [10  $\mu$ M in  $\text{CH}_3\text{CN}/\text{DMSO}$  (9:1), room temperature] of (a) the [2]rotaxane **1**, (b) the [2]rotaxane **2**, and (c) the dumbbell-shaped molecule **6** in the presence of  $\text{Bu}_4\text{NOMs}$  (0–300 eq).

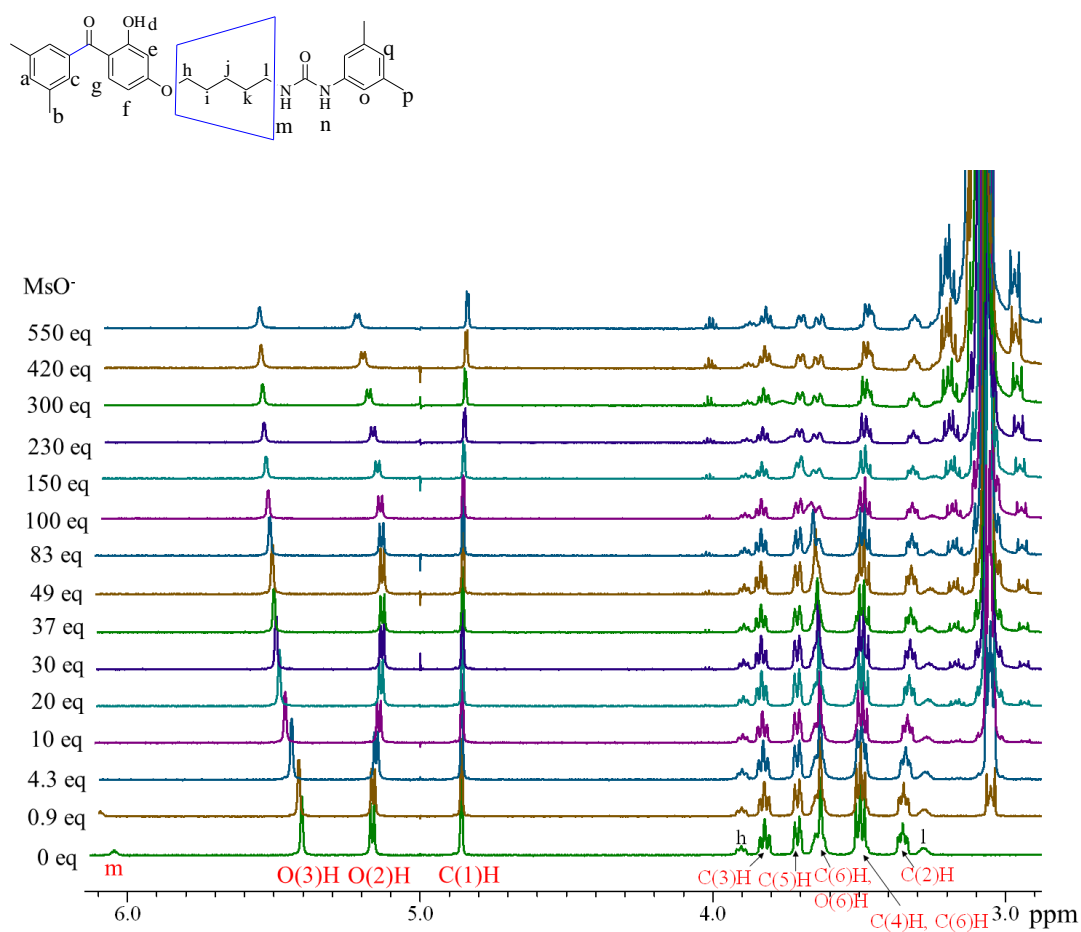


**Figure S12a.** Partial  $^1\text{H}$  NMR spectra [600 MHz,  $\text{CD}_3\text{CN}/\text{DMSO}-d_6$  (9:1), 25  $^\circ\text{C}$ ] of the [2]rotaxane **1** (0.5 mM) in the presence of  $\text{Bu}_4\text{NOMs}$  (0–550 eq).



**Figure S12b.** Simulation of titrations of the [2]rotaxane **1** and  $\text{Bu}_4\text{NOMs}$  using BindFit.

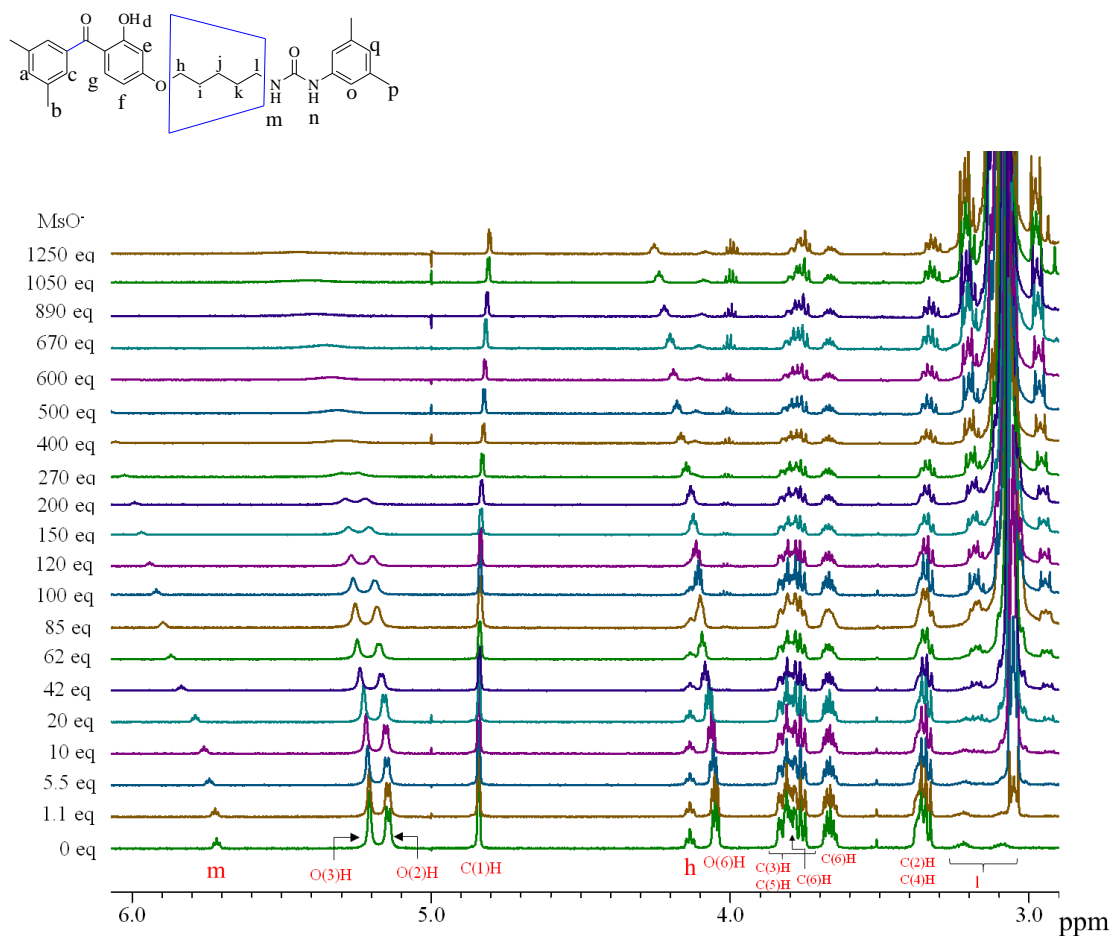


**Figure S13a.** Partial  $^1\text{H}$  NMR spectra [600 MHz,  $\text{CD}_3\text{CN}/\text{DMSO}-d_6$  (9:1), 25  $^\circ\text{C}$ ] of the [2]rotaxane **2** (0.5 mM) in the presence of  $\text{Bu}_4\text{NOMs}$  (0–1250 eq).

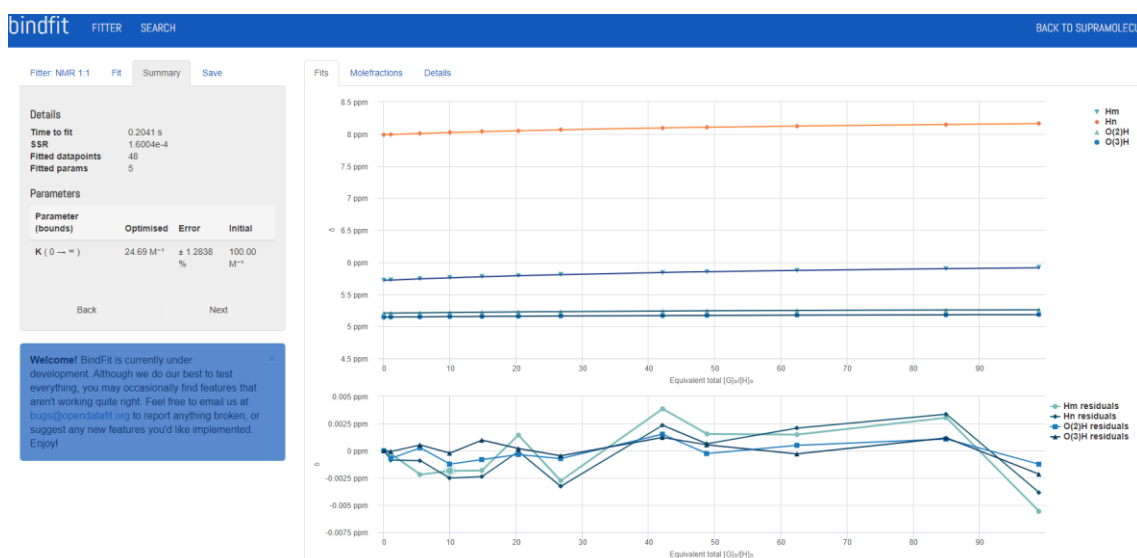


**Figure S13b.** Simulation of titrations of the [2]rotaxane **2** and  $\text{Bu}_4\text{NOMs}$  using BindFit.

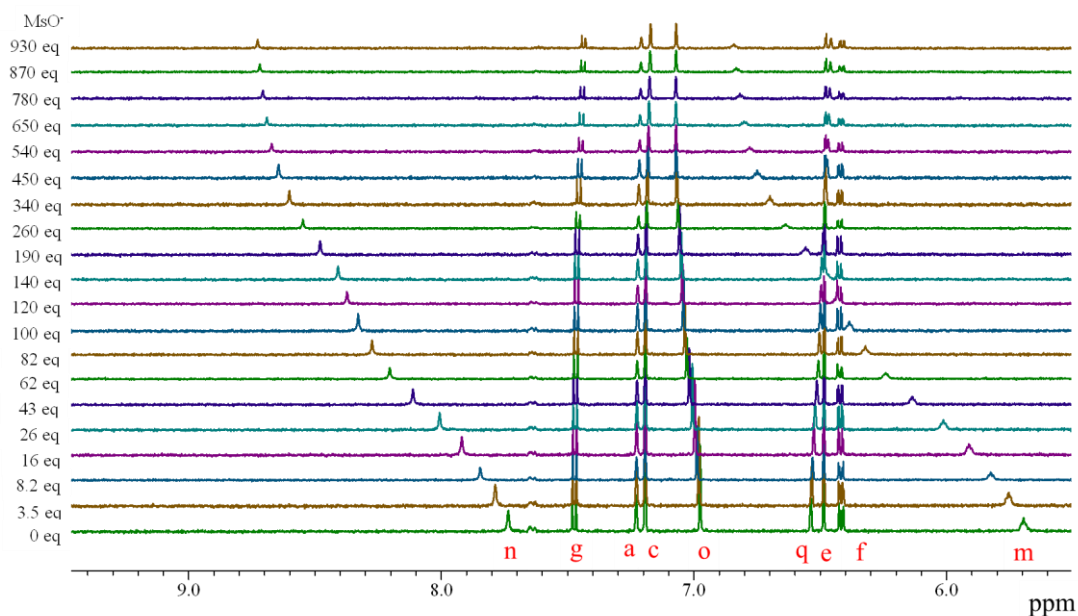
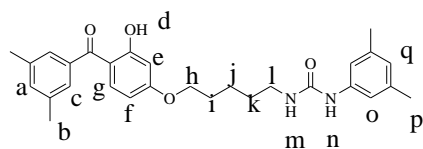


**Figure S14a.** Partial  $^1\text{H}$  NMR spectra [600 MHz,  $\text{CD}_3\text{CN}/\text{DMSO}-d_6$  (9:1), 25  $^\circ\text{C}$ ] of the dumbbell-shaped molecule **6** (0.5 mM) in the presence of  $\text{Bu}_4\text{NOMs}$  (0–930 eq).

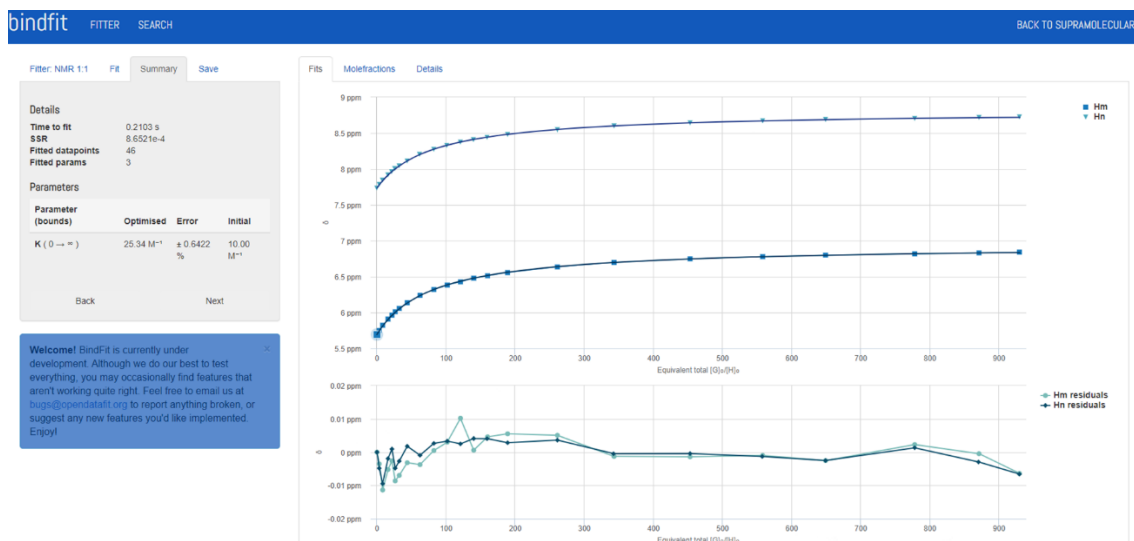


**Figure S14b.** Simulation of titrations of the dumbbell-shaped molecule **6** and  $\text{Bu}_4\text{NOMs}$  using BindFit.

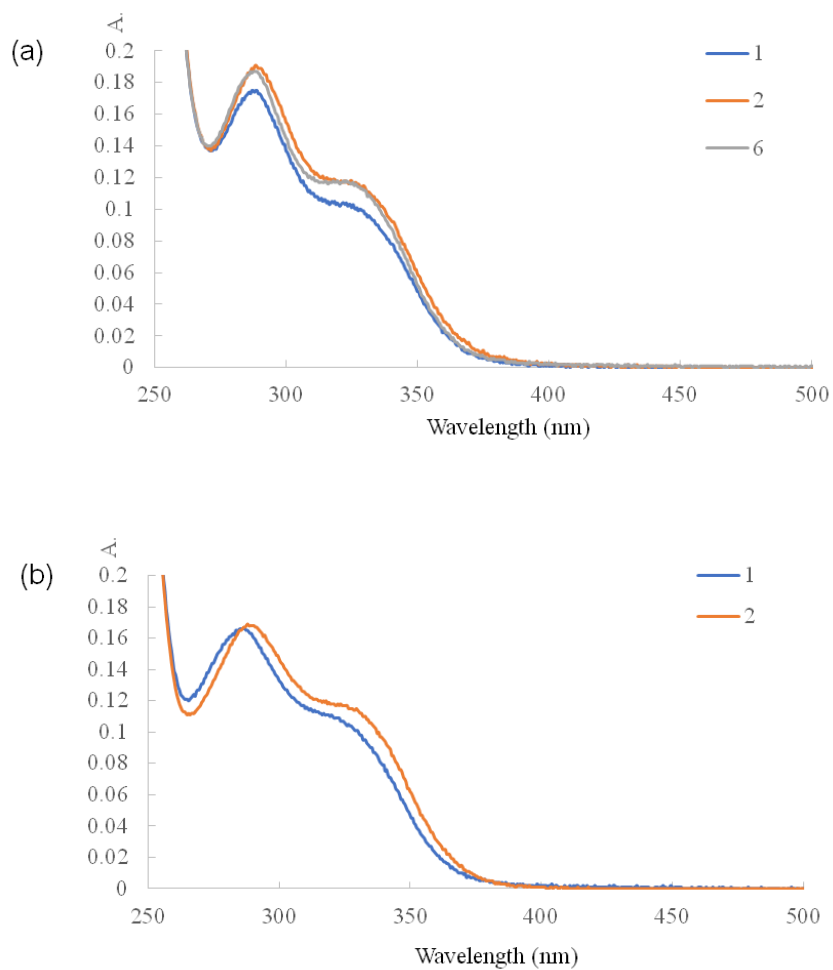


**Figure S15.** UV/Vis absorption spectra of (a) the [2]rotaxanes **1**, **2**, and the dumbbell-shaped molecule **6** [10  $\mu$ M in CH<sub>3</sub>CN/DMSO (9:1), room temperature] and (b) the [2]rotaxanes **1** and **2** [10  $\mu$ M in H<sub>2</sub>O/DMSO (9:1), room temperature].

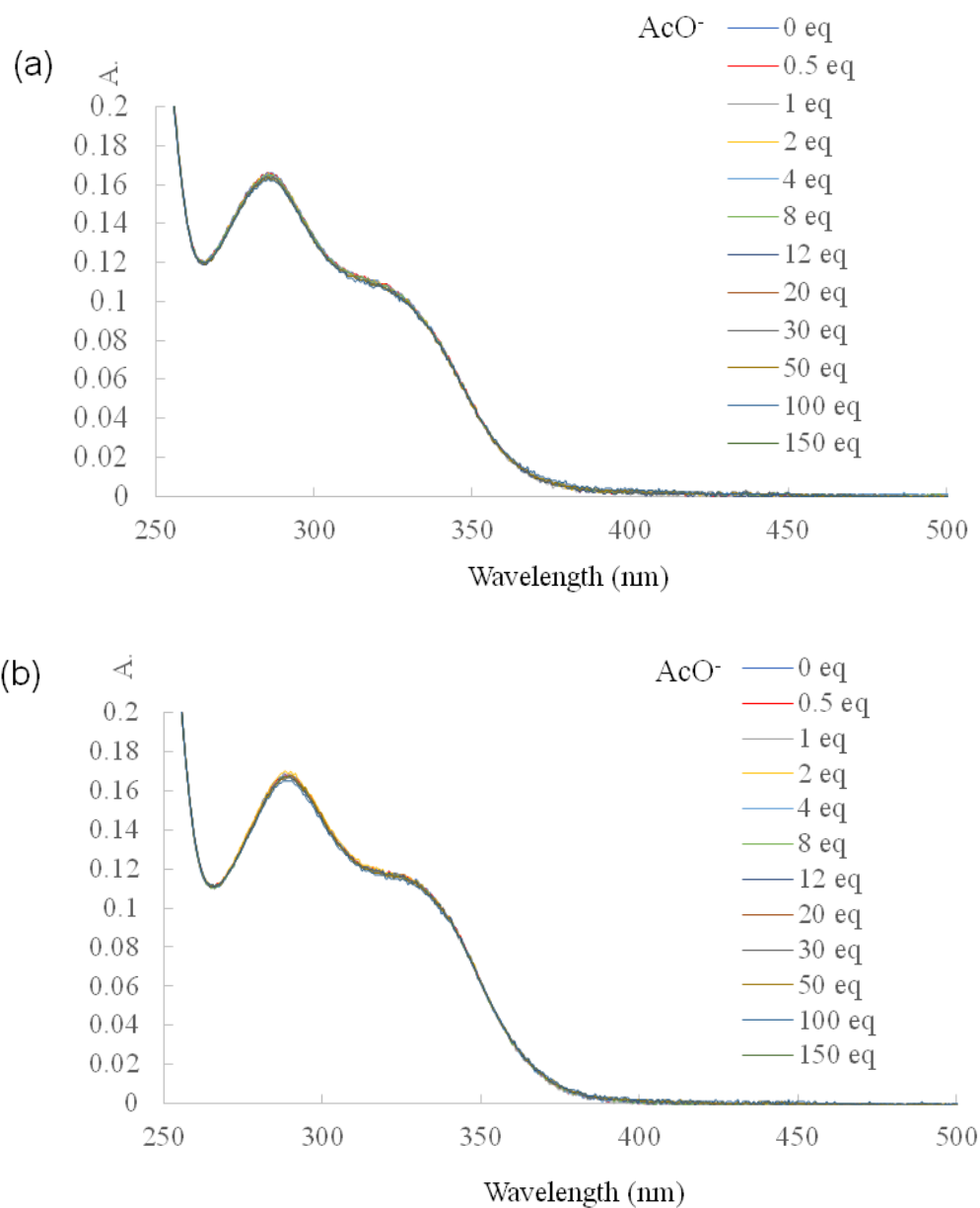


**Figure S16.** UV/Vis absorption spectra [10  $\mu$ M in H<sub>2</sub>O/DMSO (9:1), room temperature] of (a) the [2]rotaxane **1** and (b) the [2]rotaxane **2** in the presence of Bu<sub>4</sub>NOAc (0–150 eq).

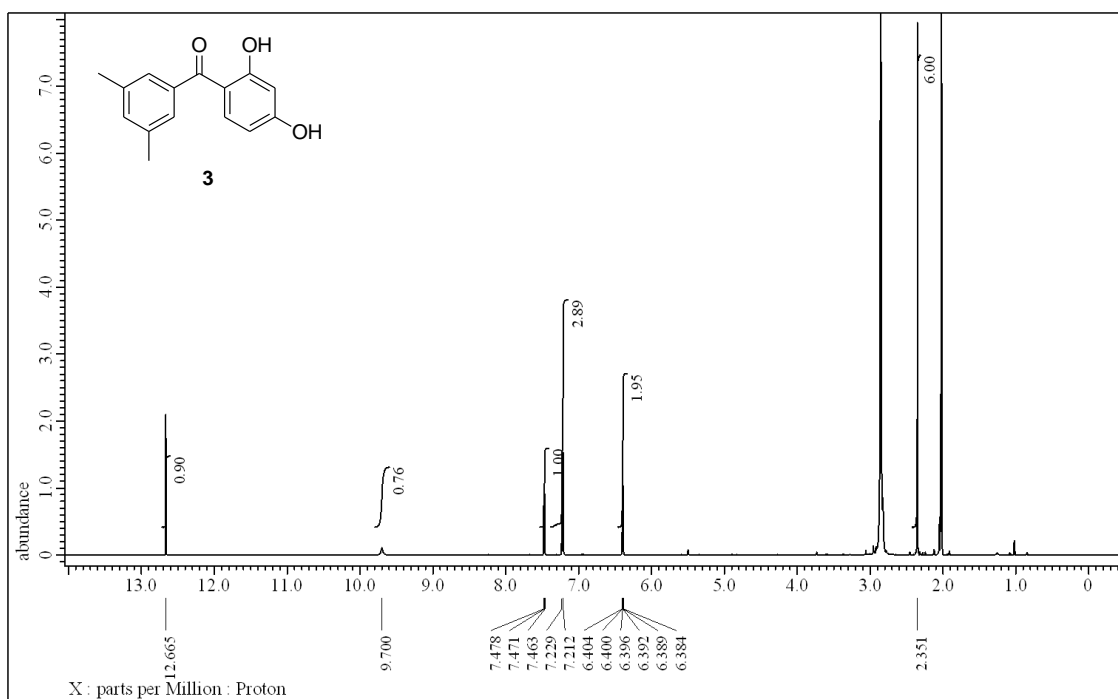


**Figure S17a.** <sup>1</sup>H NMR (600 MHz, acetone-*d*<sub>6</sub>) spectrum of compound **3**.

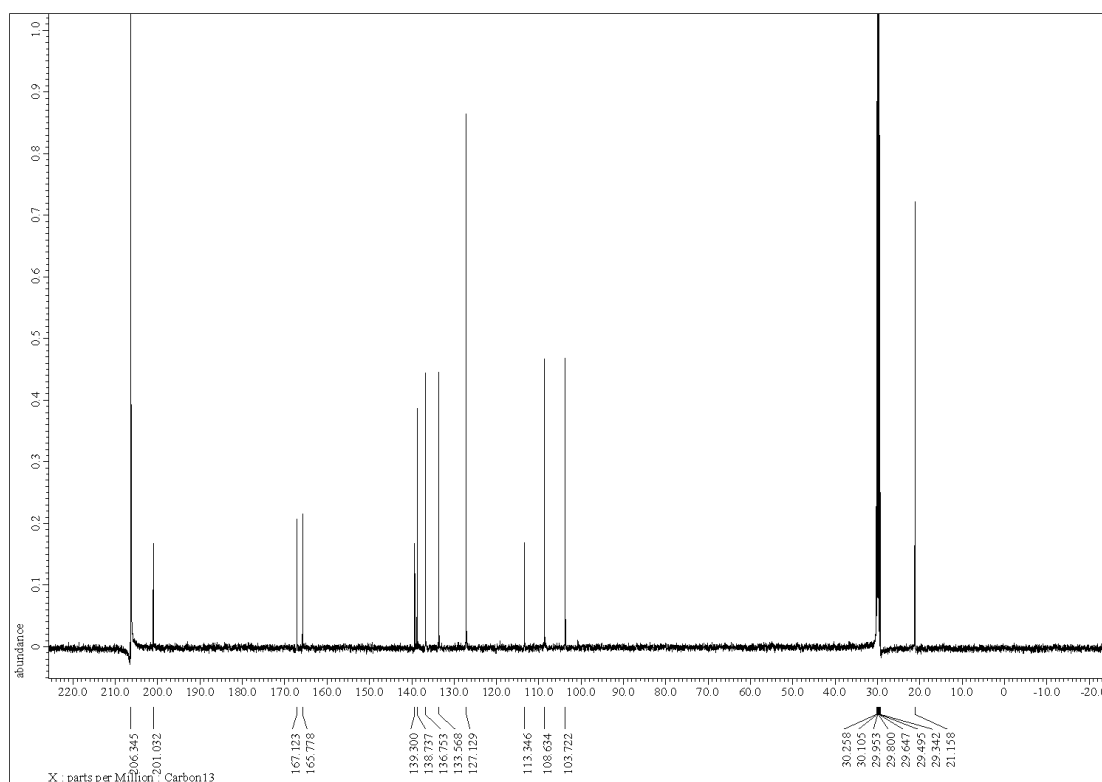


**Figure S17b.** <sup>13</sup>C NMR (125 MHz, acetone-*d*<sub>6</sub>) spectrum of compound **3**.

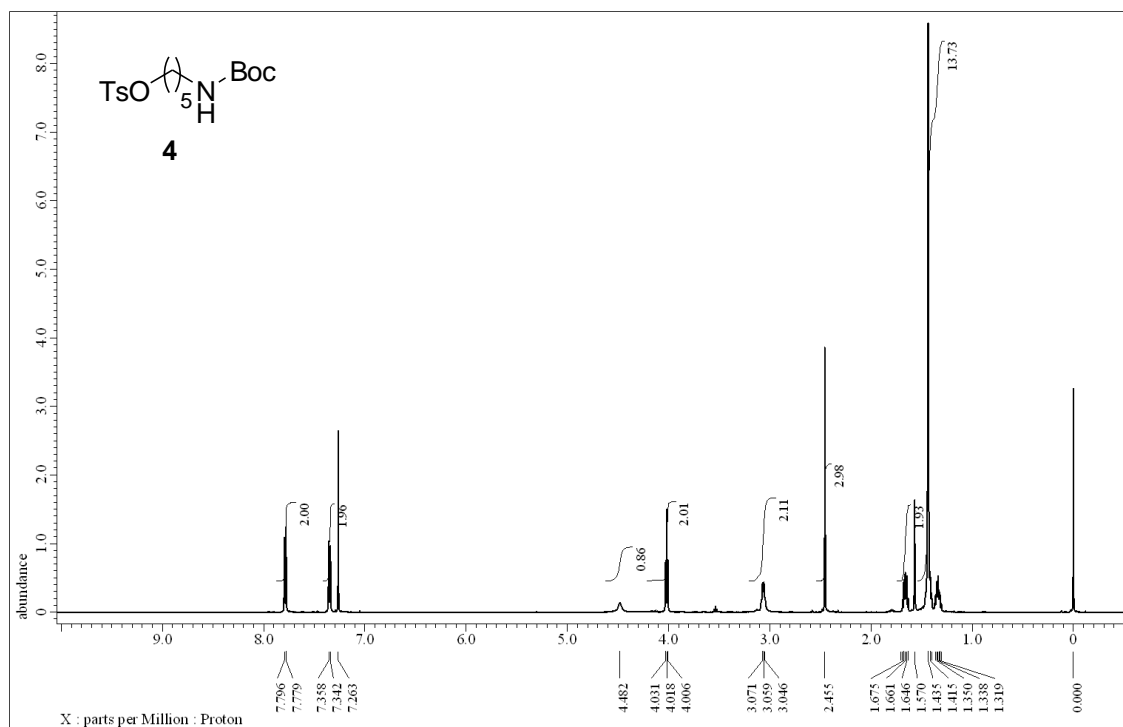


**Figure S18a.**  $^1\text{H}$  NMR (500 MHz,  $\text{CDCl}_3$ ) spectrum of compound **4**.

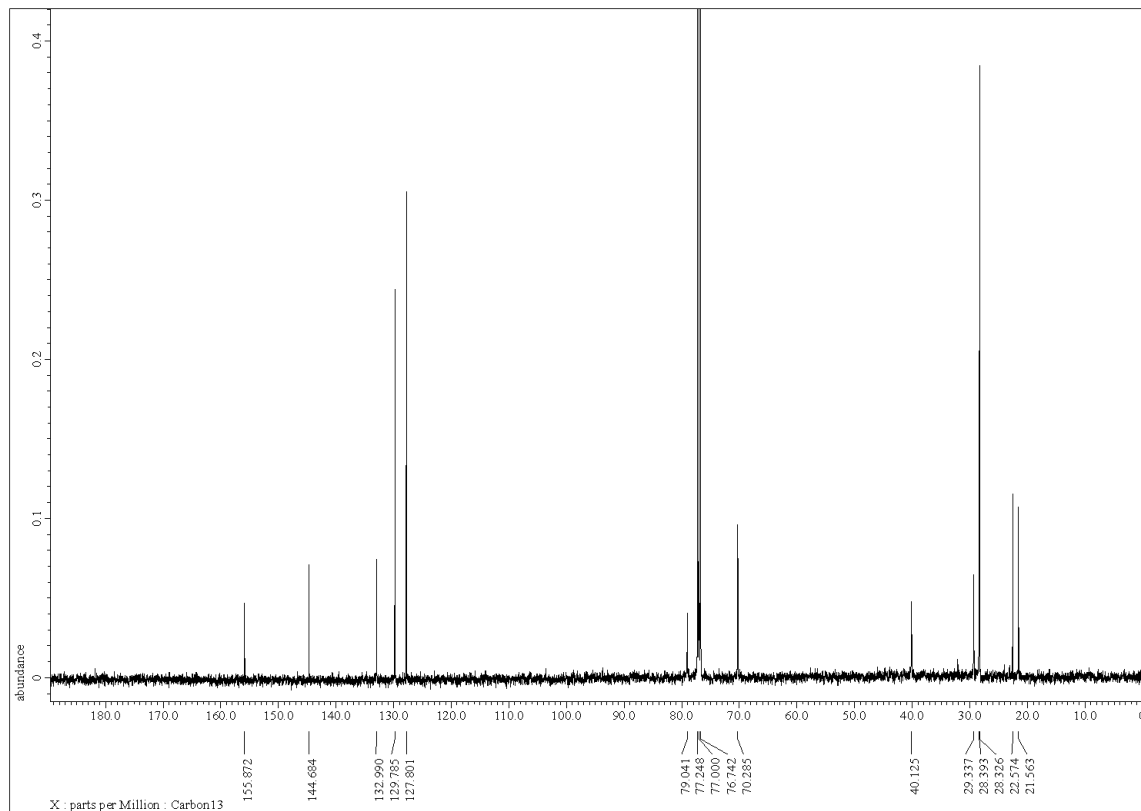


**Figure S18b.**  $^{13}\text{C}$  NMR (125 MHz,  $\text{CDCl}_3$ ) spectrum of compound **4**.

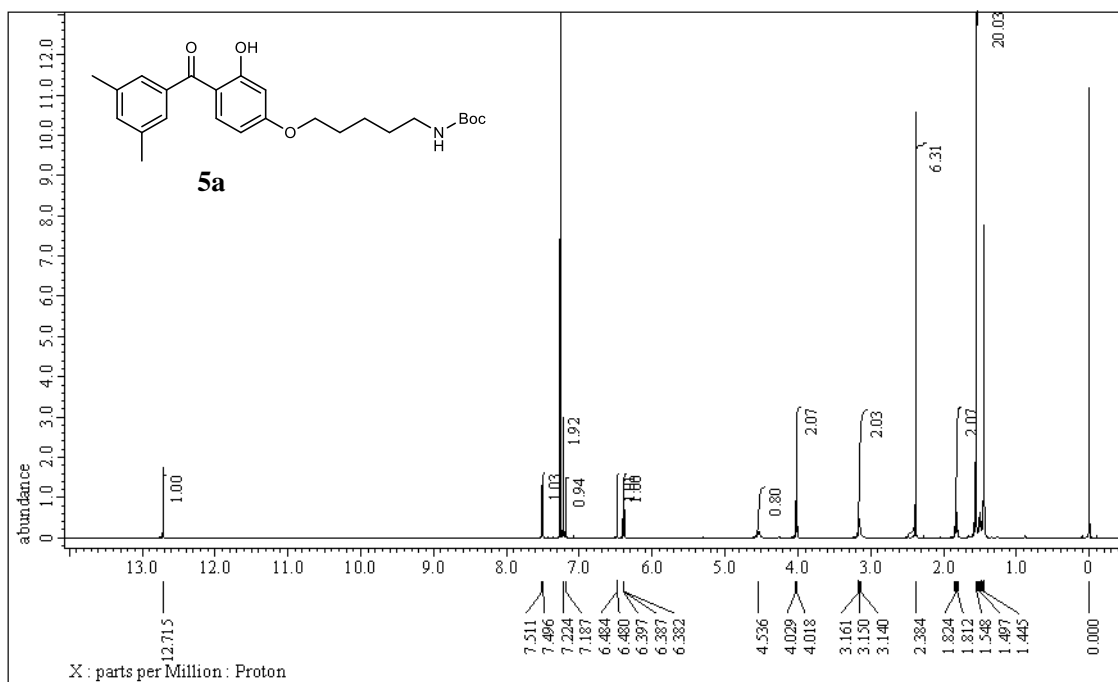


**Figure S19a.**  $^1\text{H}$  NMR (600 MHz,  $\text{CDCl}_3$ ) spectrum of compound **5a**.

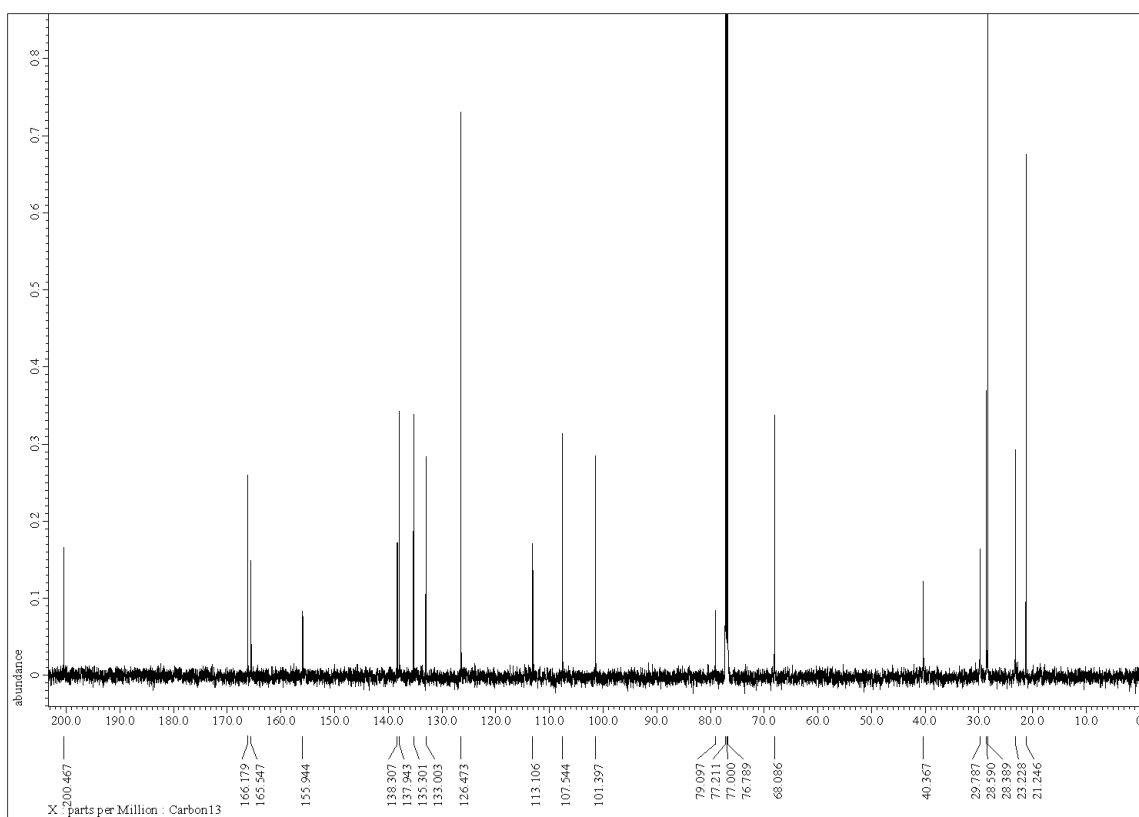


**Figure S19b.**  $^{13}\text{C}$  NMR (150 MHz,  $\text{CDCl}_3$ ) spectrum of compound **5a**.

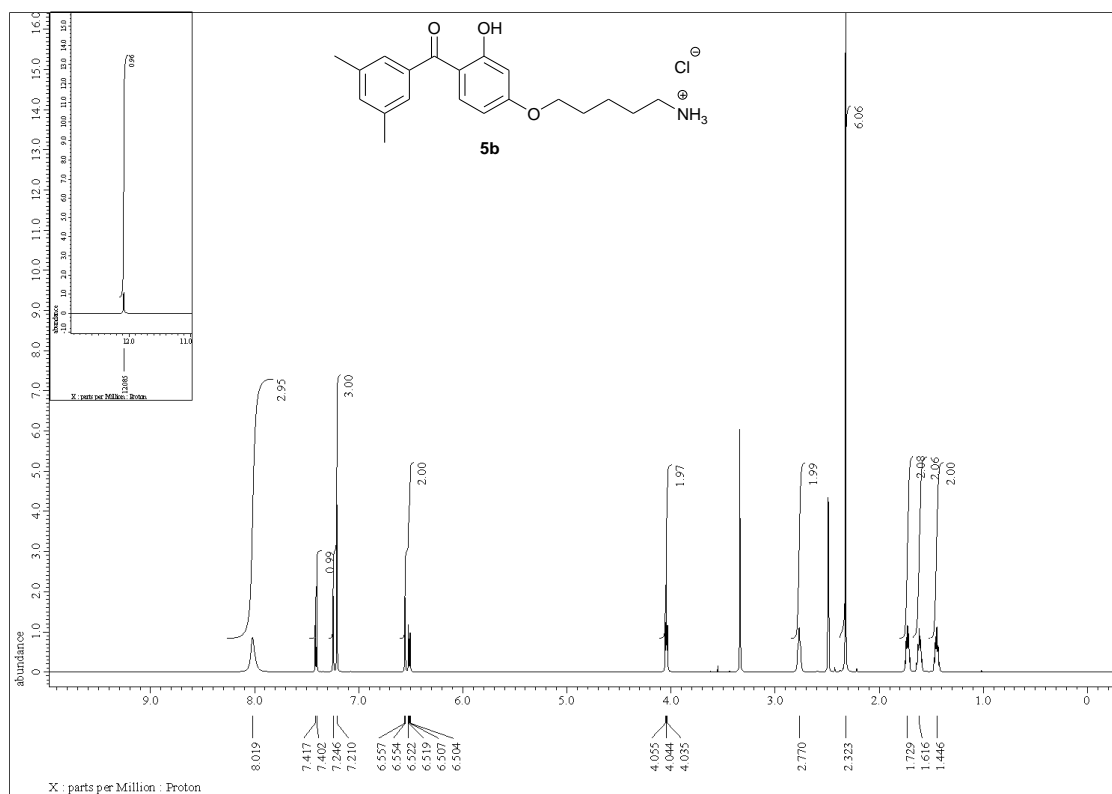


**Figure S20a.** <sup>1</sup>H NMR (600 MHz, DMSO-*d*<sub>6</sub>) spectrum of compound **5b**.

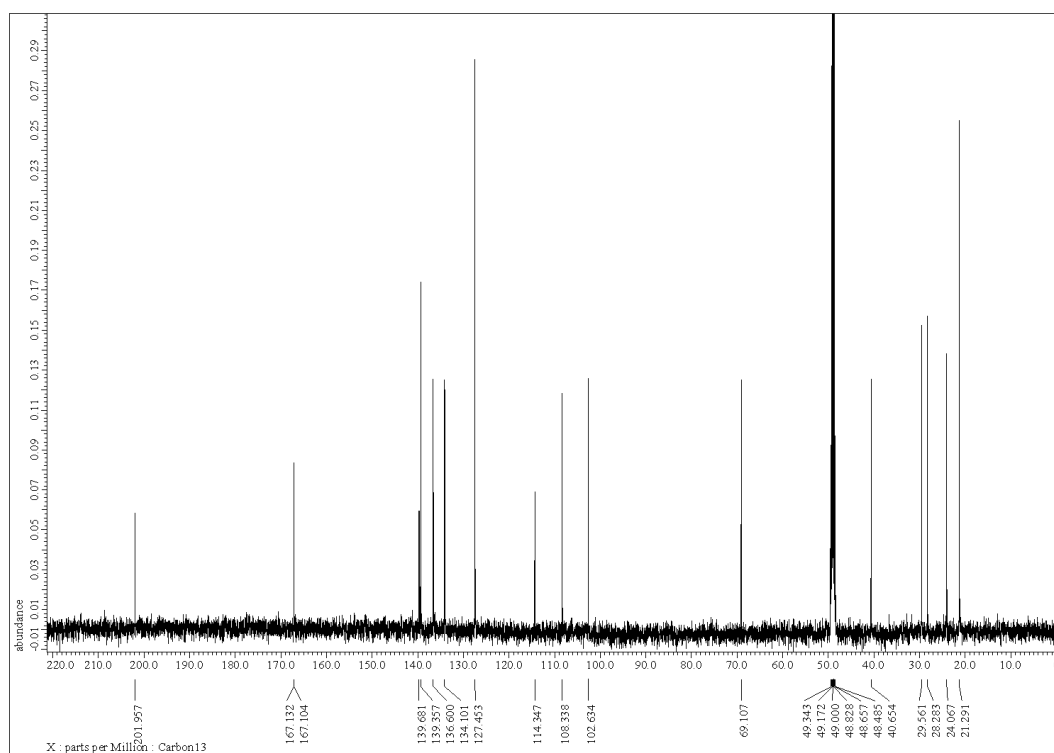


**Figure S20b.** <sup>13</sup>C NMR (125 MHz, CD<sub>3</sub>OD) spectrum of compound **5b**.

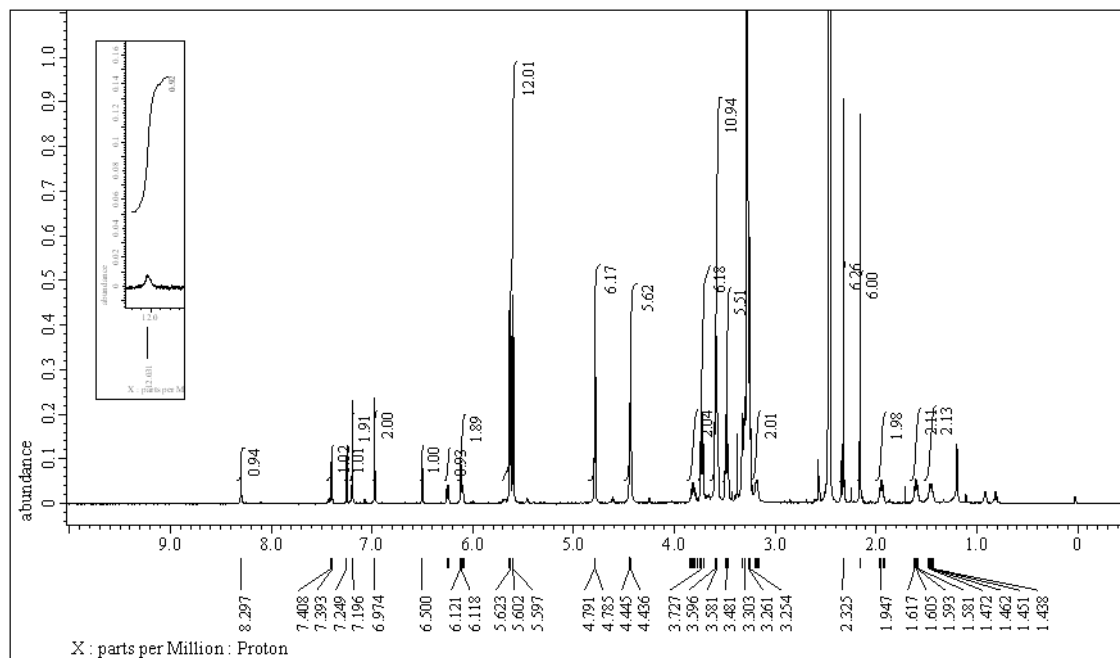
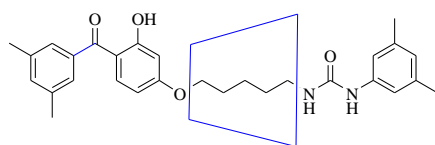


**Figure S21a.**  $^1\text{H}$  NMR (600 MHz,  $\text{DMSO-}d_6$ ) spectrum of the [2]rotaxane **1**.

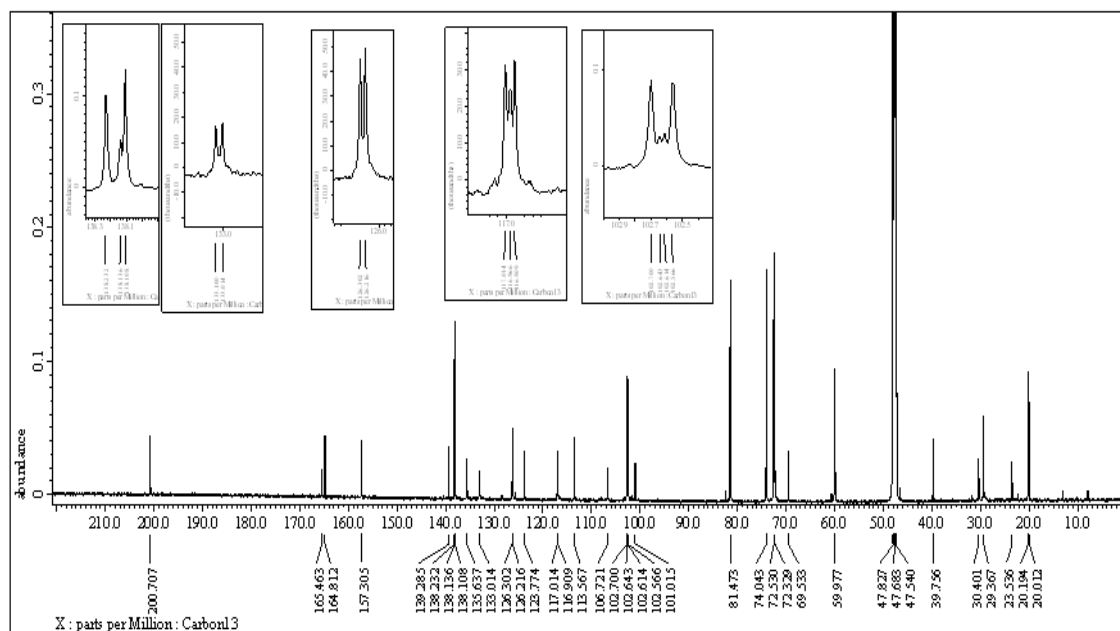


**Figure S21b.**  $^{13}\text{C}$  NMR (150 MHz,  $\text{CD}_3\text{OD}$ ) spectrum of the [2]rotaxane **1**.



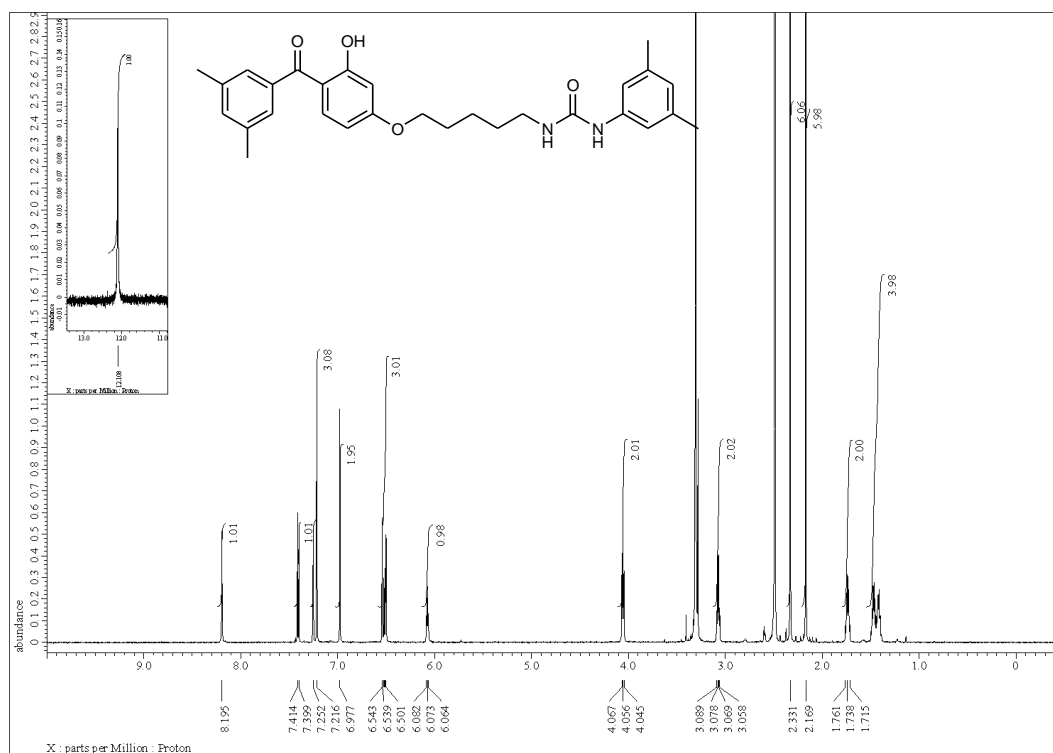


**Figure S23a.**  $^1\text{H}$  NMR (600 MHz,  $\text{DMSO-}d_6$ ) spectrum of the dumbbell-shaped molecule **6**.

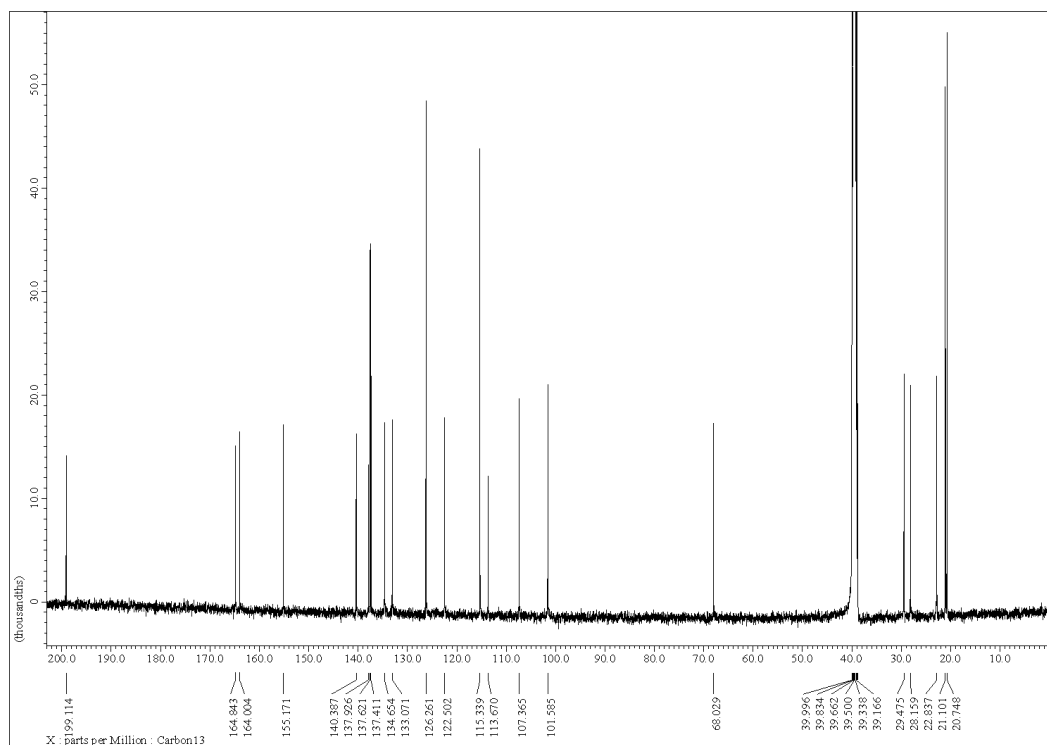


**Figure S23b.**  $^{13}\text{C}$  NMR (125 MHz,  $\text{DMSO-}d_6$ ) spectrum of the dumbbell-shaped molecule **6**.